SPE 165141

Impact of Charge Type Used in Perforation on the Outcome of Matrix Acid Treatment in Carbonate Formations: Comparative Study

Ahmed I. Rabie, and Hisham A. Nasr El-Din, Texas A&M University, and John T. Hardesty, SPE, Nathan G. Clark, SPE, and Matthew R.G. Bell, SPE, GEODynamics, Inc.

This paper was prepared for presentation at the SPE European Formation Damage Conference and Exhibition held in Noordwijk, The Netherlands, 5–7 June 2013.

Abstract

Perforation is the most common way to establish effective communication between the reservoir and the wellbore in wells completed with casing. Although perforation with shaped charges has become the dominant method for completion, conventional shaped charges do not always provide deep and clean-enough tunnels that result in the required productivity and/or facilitate subsequent stimulation treatments.

Therefore, the objectives of this work are to utilize the Perforation Flow Cell (PFC) and the Perforation Treatment Cell (PTC), both developed by GEODynamics, to investigate the impact of using reactive liner shaped charges on the outcome of matrix acidizing treatments and to compare the performance of reactive and conventional charges for different charge types and loads.

Cream Chalk cores with 7 in. diameter x 24 in. length were perforated with two weights of reactive and conventional charges (15 and 23 g) under simulated downhole conditions using two designs of charges; deep penetration (DP) and good hole (GH). All cores were initially saturated in odorless mineral spirit (OMS) and the same fluid was used to flush the core before and after the acidizing step. Porosity and pre-shot (initial) permeability were measured.

After perforation, post-shot permeability was reported and the cores were CT-scanned to visualize and measure the geometry of the perforation tunnels. 15 wt% HCl was used for the acidizing step at 200°F and the effluent samples were periodically collected to measure Ca, Mg, Fe, Al, and metal ions that are present in the core, tubulars, cement, and shaped charge material in the perforation assembly. Cumulative acid pore volume and acid injectivity were reported. CT scans were performed again after acidizing to assess the wormhole morphology obtained with various types of charges.

Experimental results showed that reactive charges create tunnels with more effective (open) length when compared to the equivalent conventional charge, especially at the tip of the tunnel. As a result, stimulation treatments were enhanced and less acid pore volume and time to breakthrough were required. These results were confirmed by chemical analysis that showed higher calcium and metal ion concentration in the effluent samples when the conventional charge was used. CT-scanning after treatment showed a dominant wormhole created from the tip of the perforation tunnel when the reactive charges were used compared to multiple and deviated/branching wormholes with the conventional charges

Introduction

Communication between a producing formation and wells completed with casing is re-established through perforation. In normal conditions, perforations become the critical conduits for production or fluid injection. Effective perforation is one that is deep enough to bypass the drilling-damage zone and clean enough to avoid restricting flow in the near-wellbore area. However, quality of perforation tunnels, in general, depends on other parameters such as perforation diameter, distribution and conditions of any materials inside the perforation tunnel, thickness of the crushed zone around the perforation, and geometry and condition of the tunnel at the tip (Bell et al. 2008a).

It has been recognized that optimizing the perforation process is a complicated multi-task process that requires a proper understanding of the interaction between formation rock, reservoir fluids, well bore conditions, and gun and hardware systems (Bell et al. 1972; 1995; Walton et al. 2001; Grove at al. 2011).

Bell et al. (1995) stated that the critical factors or properties to be considered when optimizing perforation performance can be broadly categorized in the following four areas, each of which includes multiple parameters: Reservoir and formation properties (rock mechanical properties, stress conditions, permeability, porosity, heterogeneity, and formation fluid properties), Near-wellbore formation and flow conditions (drilling fluid invasion and particle migration, laminated or

turbulent flow), Well and wellbore conditions (wellbore geometry, tubing and cement specifications, wellbore fluid properties, wellbore orientation and deviation, wellbore fluid pressure condition with respect to reservoir fluid pressure), and charge, gun and tool string system (charge type and size, gun type and size, phasing and shot density).

Optimization of perforation performance based on the aforementioned parameters requires a selection between several system design and operational options such as the initial state of relative pressure between the wellbore and the formation (i.e. under-, at-, or over-balance), perforation technique and tools, and the type and weight of the shaped charges (including conventional versus reactive charge type).

Regarding the perforation pressure conditions, several research and field studies have shown that perforating underbalanced provides an effective method for obtaining a greater proportion of clean perforations. Bonomo and Young (1983) reported that in underbalance perforating, the pressure differential from the formation to the wellbore helps remove crushed formation material from the perforation more successfully than perforation washing or surging. Bell (1982; 1984) introduced the first attempt to predict necessary underbalance pressures on the basis of permeability and well performance and reported that at least 500 psi pressure difference is necessary for perforation cleanup.

King et al. (1986) used data from 90 oil and gas wells and showed a minimum underbalance line separating the data sets of wells that had clean perforation (were not improved by post acidizing treatments) from those wells that showed a significant productivity increase after acidizing. In addition, the underbalance, necessary to achieve 'clean perforations', was shown to decrease with increasing formation permeability. They proposed flow through the formation matrix to be the mechanism of perforation cleanup. Accordingly, high permeability rocks would more readily clean-up while very low permeability rocks may not clean-up regardless of the pressure differential.

Walton (2000) proposed a different theory in which the perforation cleanup mechanism occurs because of a mechanical failure of the damaged zone. In his theory, the optimum underbalance pressure is believed to depend more on the effective stress, the strength of the rock, and the strength and extent of the perforation damaged zone.

Subiaur et al. (2004) investigated the extent to which the correlations for underbalance-perforating cleanup, based on sandstone experiments, may be applicable to carbonates. Laboratory flow tests performed with limestone and dolomite cores revealed that perforation skins are not well described by the earlier sandstone correlations based on rock permeability, but rather are best related to peak underbalance pressure and rock strength.

Since their introduction in the 1950's, perforating using shaped explosive charges has become the most common method for connecting a cased-and-cemented completion to the desired reservoir interval (Bell 2008a). The dominant use of shaped charges is because of the relative speed and simplicity of their deployment compared to alternatives, such as mechanical penetrators or hydro-abrasive jetting tools (Bell et al. 2008b).

A new class of shaped charge, known as reactive liner shaped charges or reactive perforating, was introduced to the industry in late 2007, which exploits a highly-exothermic secondary reaction in the perforation tunnel immediately after it has been formed. The reaction generates a pressure spike that drives the break up and expulsion of crushed zone material and compacted debris into the wellbore resulting in profoundly cleaner, more effective tunnels, and enhances the ease and reliability with which the perforated formation can be stimulated (Bell et al. 2009). Reactive liner shaped charges have been tested in the laboratory using stressed rocks under simulated downhole conditions and have been applied in the field with excellent results, especially as seen during fracturing treatments in terms of reduction in breakdown pressure and subsequent treating pressures (Hardesty et al. 2011a; 2011b).

For matrix acidizing it has generally been assumed that deep perforations are appropriate and that the stimulation will offset any impact of perforation damage (i.e. the acid-created wormhole will bypass the damaged zone). As discussed earlier, previous work (King et al. 1986, Subiar 2004) showed that clean perforations are related to more successful acidizing. Other work showed that injection rate and pressure can be improved if clean perforations are achieved.

Bartko et al. (2007) initiated a lab study that looked into the impact of perforating on matrix acid stimulation in carbonates by creating perforations in stressed rock followed by acidizing to create wormholes. The results showed that, in low-permeability carbonate gas reservoirs, dynamic underbalance could be used to generate cleaner and wider perforation tunnels, which in turn resulted in lower acid injection pressures and promoted dominant wormhole formation. The authors also showed that perforating with acid in the wellbore increased acid injectivity and a preferred path could be created by the acid during perforating, which triggered subsequent acid stimulation flow and resulted in a more dominant flow channel.

Diaz et al. (2010) conducted a laboratory study in which chalk cores of 20 in. length and 4 in. of diameter were perforated with reactive liner shaped charges and then acidized to breakthrough. Injectivity was found to be higher for cores perforated with reactive liner shaped charges and slightly less acid pore volume was required to break through the cores. Fluid analysis would be required to confirm the observed pressure behavior and to give more insight into the reactive charge's influence.

The objectives of this work are to: (1) utilize a Perforation Flow Cell (PFC), developed by GEODynamics, to investigate the effect of using reactive liner shaped charges on the outcome of matrix acidizing treatments and (2) compare the performance of stimulations performed afer perforating with reactive liner and conventional shaped charges through complete fluid analysis and CT-scan imaging before and after the acidizing treatments.

Experimental Studies

Materials

Cream Chalk cores (7 in. diameter x 24 in. length) were used in this study. Chemical comopsition showing the lithology of a core sample was measured using XRF technique and is shown in **Table 1**. Initial permeability and porosity were measured as described in the following section and as listed in **Table 2**. 15 wt% HCl acid solutions with 1 vol.% corrosion inhibitor were used for the acidizing experiemnts. Acid solutions were prepared by dilution from 31.45 wt% concentrated Muriatic acid and distilled water.

Perforation Flow Cell

GEODynamic built and developed the Perforation Flow Cell (PFC) to provide a tool for perforation geometry and basic flow evaluation, as shown in **Fig. 1**. The cell was used for perforation of the cores and to measure the initial (pre-shot) and post-shot permeability before and after the acidizing experiments. Various initial perforation conditions can be applied to the target sample and the cell accommodates tests at up to 10,000 psi confining and 5,000 psi wellbore and pore pressures, with targets diametres between 5 and 9 in.). Flow testing, both pre-shot and post shot, is conducted with back pressure to minimize pressure fluctuation effects.

Each of the 7 in. diameter by 24 in. length targets was first dried to constant weight and then vacuum-saturated with odorless mineral spirits (OMS). The target was placed in the core fixture and the axial permeability was measured at 7000 psi overburden and 3000 psi back pressure. The shaped charge was then loaded in a simulated gun inside the wellbore fixture, and pressures were raised to establish desired test conditions. In all test series, overburden, pore, and wellbore pressures were 7000, 3000, and 3000 psi, respectively. Therefore, all perforations were created at balanced conditions under 4000 psi of effective stress.

The shaped charge was detonated, and the pressures were allowed to equalize. The free gun volume was similar to that found in production guns (appropriate for each shaped charge), and was sized with the rest of the system to generate minimal dynamic under- or over-balance. The resulting perforations were tested for production flow performance at a standard set of flow rates. Flow rate, temperature, and pressure drop were measured, and nondimensionalized by the initial flow performance of the target to provide a standard Production Ratio (PR). The length of the perforation tunnel within each core was measured using CT-scan imaging before acidizing. Data for the post-shot stage is listed in Table 2.

Acidizing Loop

GEODynamics has also developed an Perforation Treatment Cell (PTC), shown in **Fig. 2**, to conduct the acidizing experiements. The acidizing cell includes a syringe pump connected to an OMS accumulator that injects fluid through the core during pre- and the post-flush stages and serves as the driving mechansim for injecting acid through the core during the acidizing stage. A back pressure regulator is used to keep a back pressure of 1200 psi on the outlet of the core. Pressure transducers are used to measure the differential pressure across the core during the experiments at 1 second intervals.

Another pump is used to generate and provide the overburden pressure to maintain the desired effective stress of 4000 psi. Two heat exchanger loops are used to heat and cool the inlet and effluent streams, respectively. The inlet heat exchanger loop and the acidizing cell are installed inside an electric oven to provide the temperature necessary for the experiemnts that were conducted at 200°F. Three thermocouples were used to measure the inlet, outlet, and vessel skin temperatures of the acidizing cell.

Experimental Procedure for Acidizing Experiments

Referring to Fig. 2, acid solution is first loaded into the Acid Reservoir using a manually-controlled pump. The remotely controlled Acid Transfer Pump is then used to transfer the acid from the acid reservoir to the Acid Transfer Barrier. Acid level is monitored in the Acid Reservoir and when the required volume of the acid has been transferred, the pump is stopped.

OMS is then circulated through the lines in a core-bypass mode and the effluent is collected into the effluent reservoir to flush out any residual acid in the lines from the previous experiment. OMS injection is then switched through the core at the desired flow rate (50 cc/min) in a pre-flush stage. Temperature is brought up to 200°F and kept the same for all other experiments. After stabilization, several loop valves are controlled to direct the OMS flow to the upstream side of the Acid Transfer Barrier. This in turn pushes acid through the core for acidizing. Once acid injection has begun, samples are collected downstream of the cooling heat exchanger loop as shown in **Fig. 3**. Through the whole process of OMS or acid injection, inlet and outlet pressure, inlet, outlet, and skin-vessel temperatures, and flow rate are all recorded as a function of time. Acid is injected until breakthrough, at which point flow is switched back to OMS for a post-flush stage.

Results and Discussion

In order to investigate the effect of perforation design on subsequent acidizing treatments and specifically to compare the performance of reactive liner and conventional shaped charges and their impact on acid consumption and wormhole structure, two charge weights (15 and 23 grams) and two charge designs; Good Hole (GH) and Deep Penetration (DP), were examined for each charge type.

The body of the experimental study can be divided into three groups with a total of 6 cases of a single shot perforation followed by acidizing till the breakthrough, as shown in **Table 3**. Group 1 comprises 2 cores that were perforated using 23-ram reactive liner and conventional charges with Good Hole (GH) designs. Group 2 represents the results of acidizing 2 cores with 23-gram conventional and reactive liner charges with Deep Penetrating (DP) designs. Group 3 shows the results of the last 2 cores which were perforated using 15-gram charges with DP designs. The following discussion explains the results observed in each case and highlights the main differences between the three groups.

Group 1: Good Hole Perforation Charges

Under this category, two experiments were conducted using a charge load of 23 grams. Core CTS-20 was perforated using a reactive liner shaped charge and core CTS-11 was perforated with a conventional charge. The cores were loaded in the Perforation Flow Cell (PFC) and shot at balanced conditions and 4000 psi effective stress.

For Core CTS-20, the initial permeability was 14.3 mD and the post-shot permeability prior to acidizing was 19.9 mD. The core was then loaded into the acidizing cell and 15 wt% HCl solution with 1 vol.% of a corrosion inhibitor was injected at a rate of 50 cc/min at 200°F. From the moment of acid injection, 20 samples were taken periodically in time.

Clear OMS was observed in the first 6 samples, while sludge and dark green-to-brown fluid was observed in samples 7 to 12. Another clear phase of OMS was then observed from sample 13 to sample 20. It was clear that samples 7-12 contained two phases (acid phase and OMS phase).

Because these samples contained 2 immiscible phases, separation of the phases was performed before fluid analysis. A 6-tube centrifuge was used at a speed of 3000 rpm for 10 minutes to separate the two phases. It was noted that the sludge was mainly contained within the OMS phase. The clear acid phase was subjected to fluid analysis in which the concentration of the following ions in the effluent samples was measured using induced coupled plasma (ICP): calcium, magnesium, iron, aluminum, tungsten, and lead.

Acid injection continued for about 6 minutes and consumed a total of 0.315 acid pore volumes prior to breakthrough. The acid pore volume was determined based on the unperforated core length, therefore the effect of having different lengths of perforation tunnels should be minimized. **Fig. 4** illustrates the pressure drop across core CTS-20 as a function of the cumulative acid pore volumes pumped. Through the first 0.15 acid pore volumes, the acid was trying to enter the core from only the face of the perforation tunnel as the rest of the core inlet surface was shielded. The first drop in pressure occured once the acid was able to flow through the perforation tunnel and dissolve the acid-soluble portion of the debris. Thereafter, the acid flowed through the non-perforated portion of the core, which required 0.05 acid pore volumes to create a wormhole and break through the core. Similar pressure behavior was found to be typical during the acidization of all other cores tested in this study.

Samples were collected every minute during the acid phase flow for chemical analysis of the effluent samples. During perforation, an assembly comprising the core, cementing material, and a metal casing plate was used to represent the downhole situation. Therefore, calcium and magnesium are expected in the fluid samples based on the chemical composition of the Cream Chalk, shown in Table 1. Iron is expected as it is the main constituent of the casing plate. Calcium, magnesium, iron and aluminum are present within the cement material. Tungsten and lead are two important constituents within the shaped charge liner.

Calcium and magnesium concentration are shown in **Fig 5**, which indicates a Ca/Mg ratio of 143 (on a weight basis). This ratio is much less than the Ca/Mg ratio (≈ 500) presented by Table 1 for the core composition, which indicates that the difference in the amount of Mg came from the cement. **Fig. 6** shows the concentration of iron and aluminum in the effluent samples, while lead and tungsten measurements are illustrated in **Fig. 7**.

Fig. 8 illustrates a longitudinal section of CT-images of core CTS-20 before and after acidizing. **Fig. 8-a** shows the perforation tunnel before acidizing, which penetrated to a length of 18.8 in. as described in Table 3. Two colors can be distinguished in the figure, blue and white. The blue color represents area with low CT-numbers indicating a clean and empty path for flow, while the white color refers to areas with high CT-number indicating a dense filling material. However, it should be noted that CT-number does not give a quantitative measurement of any material represented by any color. **Fig. 8-a** shows that most of the tunnel created by the reactive liner shaped charge in this core was clean. **Fig. 8-b** shows the core after acid breakthrough and it can be observed that a dominant single wormhole was created from the tip of the perforation tunnel.

Core CTS-11 was the second core investigated under this category. The core was perforated using the same weight and design of charge as core CTS-20 (i.e. 23 g Good Hole), however, using a conventional charge type. **Fig. 9** describes the differential pressure across core CTS-11 as a function of the cumulative acid pore volume and indicates that 0.2 PV was associated with acid flow through the perforation tunnel and a further 0.3 PV was necessary for the acid to flow through the non-perforated portion of the core until breakthrough. Although both cores showed almost identical initial (matrix) permeability, significant difference is observed in the acid consumption for matrix dissolution. This was further confirmed by analyzing the average calcium and magnesium concentration in the effluent samples for core CTS-11, shown in **Fig. 10**.

The figure shows an average of 60,000 mg/l of calcium concentration for CTS-11, compared to an average of 25,000 mg/l that was found in the effluent samples from core CTS-20. Measurements of aluminum and iron for core CTS-11 are shown in **Fig. 11** and indicate higher concentrations of these ions in the effluent samples compared to those shown in **Fig. 6** for core CTS-20. Aluminum and iron were not measured in the core lithology and are main constituents of the tubular plate and cementing material in the perforation assembly. **Fig. 12** shows the measurements of tungsten and lead.

Based on these results, it is concluded that when perforating with conventional charges, larger amounts of debris remain in the perforation tunnel, especially at the tunnel tip. The presence of this debris requires longer injection of acid to dissolve acid soluble material and overcome flow resistance in the tunnel. In addition, the plugged tunnel tip forces the acid solution to deviate and creates non-useful side branches that also consume larger volume of acid.

Fig. 13 further confirms the preceding results, which illustrates the CT-images of CTS-11 before and after acidizing. Two main wormholes were initially generated from an area above the perforation tunnel and several branches are observed on the sides of each of these two wormholes.

Group 2: Deep Penetration Perforation Charges: 23 gram Charge Load

Two cores were investigated in this category; core CTS-15 was perforated with the reactive liner shaped charge and CTS-09 was perforated using the conventional charge. The pressure differential across core CTS-15 is shown in **Fig. 14**, which indicates that about 0.07 PV of acid was necessary for matrix breakthrough. The results in this figure indicate that the acid pore volume consumed for matrix acidizing for core CTS-15 was close to that consumed in core CTS-20 in group 1. Both cores were perforated using reactive charges and both cores showed similar initial permeability and porosity. The slight increase in acid pore volume required for core CTS-15 (0.07 PV) compared to core CTS-20 (0.06 PV) is due to the difference in the length of the perforation tunnel 17.6 in. (CTS-15) vs. 18.6 in. (CTS-20).

Fig. 15 illustrates the differential pressure across core CTS-09 that was perforated using a conventional charge. It is observed that 0.37 acid pore volumes were necessary to acidize the matrix until breakthrough. This acid pore volume is consistent with the results from core CTS-11 that was perforated using the same type and weight of charges, however, using a Good Hole charge design.

Calcium and magnesium concentrations in the effluent samples for CTS-15 and CTS-09 are shown in **Fig. 16** and **Fig. 17**, respectively. Measurements of iron and aluminum concentration for both cores are illustrated in **Fig. 18** and **Fig. 19**, respectively. Higher concentrations of these elements were observed for CTS-09 than CTS-15.

Fig. 20 shows the longitudinal sections of the scanned images for core CTS-15 and CTS-09 after the acidizing and illustrates a dominant wormhole created from the tip of the perforation tunnel in core CTS-15 (reactive charge) versus several deviated and branching wormholes in core CTS-09 (conventional charge) created from above the tunnel tip. This further illustrates the importance of the condition of the tunnel tip on subsequent acidizing treatments, which is evidently more favorable when reactive liner shaped charges are used.

Group 3: Deep Penetration Perforation Charges: 15 gram Charge Load

The last group under investigation involved cores that were perforated under similar conditions to group 2, however using charges with lower explosive weights (15 grams only). Core CTS-22 was perforated using a reactive liner shaped charge, while CTS-16 was perforated using a conventional charge. The smaller load was selected in order to create shorter perforation tunnels and amplify any differences in acid reaction within the matrix beyond each tunnel. Although CT-measurements in core CTS-22 revealed a perforation tunnel with a length of 18.2 versus a 14.0 in. perforation tunnel in core CTS-16, determining the acid pore volume based on the non-perforated section will minimize this effect.

Fig. 21 indicates that 0.18 PV of acid was consumed in core CTS-22 to break through the matrix, while **Fig. 22** illustrates the pressure drop in core CTS-16 and indicates an acid consumption of 0.20 PV. The small difference in the acid consumption might appear to contradict with the results obtained in group 1 and group 2, especially because a longer perforation tunnel was created in core CTS-22. However, examination of the Ca and Mg concentrations in effluent samples taken from the two cores shows that an average of 20,000 mg/l of calcium was dissolved in each sample collected during the acidizing of core CTS-22, while 35,000 mg/l was the average calcium concentration in the effluent samples from core CTS-16. These results are shown in **Fig. 23** and **Fig. 24**, respectively. The CT-images for the acidized cores reproduced in **Fig. 25** show more deviated and branching wormholes for core CTS-16, which was perforated with the conventional charge.

Conclusions

This study investigated the impact of perforation charge selection – specifically between reactive liner shaped charges and conventional shaped charges - on subsequent acidizing treatments. A total of six single-shot tests were reported in 7 in. (D) x 24 in. (L) cores, acidized using 15 wt% HCl. The following conclusions can be drawn:

1- Initial perforation geometry produced by varied charge design has a significant effect upon the effectiveness of acid treatment for the targets and conditions within this study.

2- Reactive liner shaped charges created tunnels with more effective (open) length when compared to conventional charges, with notable improvement in tunnel quality at the tip of the tunnel.

3- Acid consumption expressed in cumulative pore volumes was higher in cores perforated with conventional charges. Effluent fluid analysis showed higher calcium, magnesium, and metal ion concentrations in effluent samples when a conventional charge was used, indicating dissolution of greater amounts of perforation debris and formation material was required to achieve breakthrough.

4- CT-scan images confirmed the preceding results by showing a dominant wormhole generated from the tunnel tip when reactive liner shaped charges were used, compared to multiple and deviated wormholes originating before the tunnel tip when conventional charges were used.

5- Perforation of carbonate formations with properly designed reactive liner shaped charges rather than conventional shaped charges should result in more effective matrix acid stimulation as dominant wormholes will be created from the tip of each perforation tunnel, resulting in greater effective wellbore radius for a given volume of acid stimulation.

Acknowledgements

The authors would like to thank GEODynamics Inc. for funding the experimental program and granting permission to publish and present this paper. The authors also wish to express their appreciation to Mr. Jarrod Pearson and Mr. Chris Pool for their committed support during the experimental work of the paper.

References

Bartko, K.M., Chang, F.F., Behrmann, L.A., and Walton, I.C. 2007. Effective Matrix Acidizing in Carbonate Reservoir-Does Perforating Matter?. Paper SPE 105022 presented at the Middle East Oil and Gas Show, Bahrain, 11-14 March.

Bell, M.R., Hardesty, J.T., and Clark, N.G. 2008. A New Technique for the Development and Quality Control of Flow-Optimized Shaped Charges. Paper presented at the Offshore Technology Conference, Houston, Texas, USA. OTC-19331-MS. DOI: 10.4043/19331-ms.

Bell, M.R.G., Hardesty J., and Clark, N.G. 2008a. A New Technique for the Development and Quality Control of Flow-Optimized Shaped Charges. Paper SPE 19331 presented at the Offshore Technology Conference, Houston, Texas, USA, 5-8 May.

Bell, M.R.G., Hardesty J., and Clark, N.G. 2009. Reactive Perforating: Conventional and Unconventional Applications, Learnings and Opportunities. Paper SPE 122174 presented at the SPE European Formation Damage Conference, Netherlands, 27-29 May.

Bell, W.T. 1982. Perforating Techniques for Maximizing Well Productivity. Paper SPE 10033 presented at the International Technical Symposium, Beijing, 18-26 March.

Bell, W.T. 1984. Perforating Underbalanced-Evolving Techniques. *JPT*, **36**(10): 1653-1662

Bell, W.T., Brieger, E.F., and Harrigan, J.W. 1972. Laboratory Characterization of Gun Perforations. *JPT*, **24**(9): 1095-1103.

Bell, W.T., Sukup, R.A., and Tariq, S.M. 1995. Perforating. *SPE Monograph*, Volume 16, Richardson, Society of Petroleum Engineering, Richardson , TX.

Bonomo, I.M. and Young, W.S. 1983. Analysis and Evaluation of Perforating and Perforation Cleanup Methods. Paper SPE 12106 presented at the 1983 SPE Annual Technical Conference and Exhibition, San Francisco, USA, 5-8 October.

Diaz, N.J., Bell, M.R.G., Hardesty, J.T., Hill, A.D., and Nasr-El-Din, H.A. 2010. An Evaluation of the Impact of Reactive Perforating Charges on Acid Wormholing in Carbonates. Paper SPE 138424 presented at the SPE Latin American and Caribbean Petroleum Engineering Conference, Lima, Peru, 1-3 December.

Grove, B., Harvey, J. and Zhan, L. 2011. Perforation Cleanup via Dynamic Underbalance: New Understanding. Paper SPE 143997 presented at the 2011 SPE European Formation Damage Conference, The Netherlands, 7-10 June.

Hardesty, J., Bell, M.R.G., Clark, N.G., Zaleski, T., and Bhakta, S. 2011a. Translation of New Experimental Test Methods for the Evaluation and Design of Shaped Charge Perforators to Field Applications. Paper SPE 144167 presented at the European Formation Damage Conference, Noordwijk, The Netherlands, 7-10 June.

Hardesty, J., Clark, N.G., Bell, M.R.G., and Zaleski, T. 2011b. Perforation Shaped Charge Design for Shale Produces Improved Tunnel Geometry. Paper SPE 149453 presented at the SPE Eastern Regional Meeting, Columbus, Ohio, USA, 17-19 August.

King, G.E., Anderson, A., and Bingham, M. 1986. A Field Study of Underbalance Pressures Necessary to Obtain Clean Perforation Using Tubing Conveyed Perforating. *JPT*, **38**(6): 662-664.

Subiaur, S.T., Graham, C.A., and Walton, I.C. 2004. Underbalance Pressure Criteria for Perforating Carbonates. Paper SPE 86542 presented at the 2004 International Symposium and Exhibition on Formation Damage Control, Lafayette, Louisiana, USA, 18-20 Febraury.

Walton, I.C. 2000. Optimum Underbalanace for the Removal of Perforation Damage. Paper SPE 63108 presented at the 2000 SPE Annual Technical Conference and Exhibition, Dallas, Texas, USA, 1-4 October.

Walton, I.C., Johnson, A.B., Behrmann, L.A., Atwood, A.C. 2001. Laboratory Experiments Provide New Insights into Underbalanced Perforating. Paper SPE 71642 presented at the 2001 SPE Annual Technical Conference and Exhibition, New Orleans, Louisiana, USA, September 30 – October 3.

Table 1: Chemical composition of Cream Chalk used in the current study using XRF technique.

Chemical composition, wt%	
Al	0.0707
C	11.9
Ca	39.7
Cl	0.2
Fe	0.0379
K	0.0233
Mg	0.0794
O	47.8
S	0.0329
Si	0.121
Sn	0.0121
Sr	0.0227
$CaCO_3$, wt%	99.4

Table 2: Porosity, initial (pre-shot) permeability, post-shot permeability, and tunnel length of the Cream Chalk cores used in the current study.

Run #	Core Number	Porosity, vol.%	Initial (Pre-shot) Permeability, mD	Post-shot Permeability, mD	Tunnel length, in.
1	CTS 09	27.2	12.3	21.2	17.1
2	CTS 11	27.4	14.4	23.8	15.8
3	CTS 15	28	15.3	34.8	17.6
4	CTS 16	27.7	14.6	16.3	14.0
5	CTS 20	27.5	14.3	19.9	18.6
6	CTS 22	28	14.0	15.6	18.2

Table 3: Summary of the coreflood results for the acidizing experiments conducted in this study.

Run #	Core Number	Type of Charge	Charge Weight, g	Length of Perforation Tunnel, in.	Acid pore Volume, (PV)
5	CTS-20	Reactive − GH	23	18.6	0.05
2	CTS-11	Conventional − GH	23	15.8	0.30
3	CTS-15	Reactive − DP	23	17.6	0.07
1	CTS-09	Conventional − DP	23	17.1	0.37
6	CTS-22	Reactive − DP	15	18.2	0.18
4	CTS-16	Conventional − DP	15	14.0	0.20

- GH: Hole Design
- DP: Deep Penetration Design

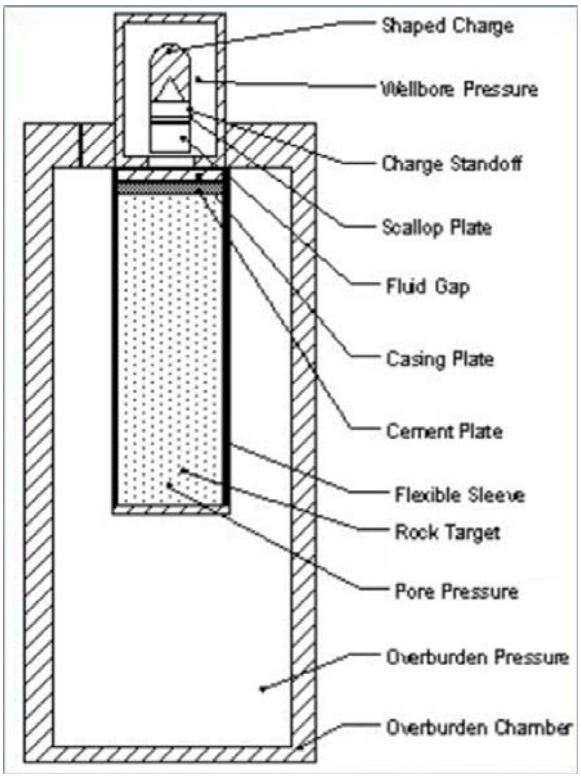

Fig. 1: A schematic diagram for the Perforation Flow Cell.

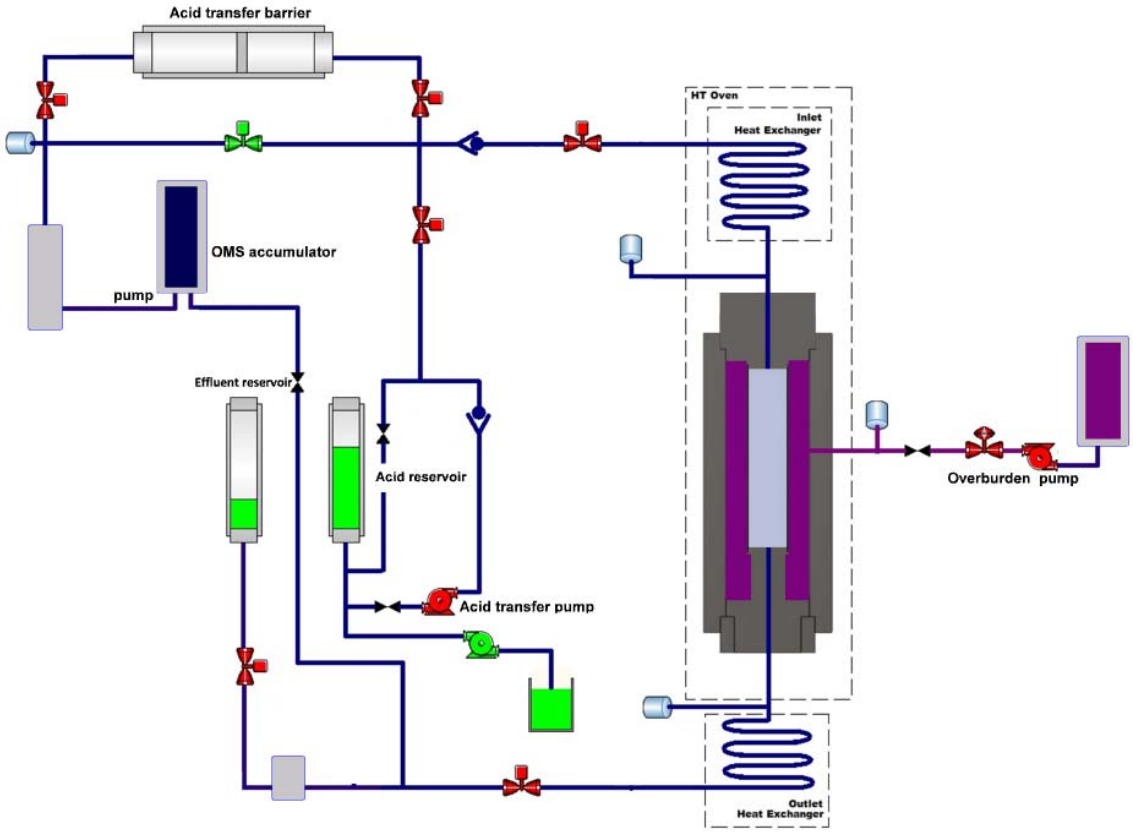

Fig. 2: A schematic diagram for the Perforation Treatment Cell.

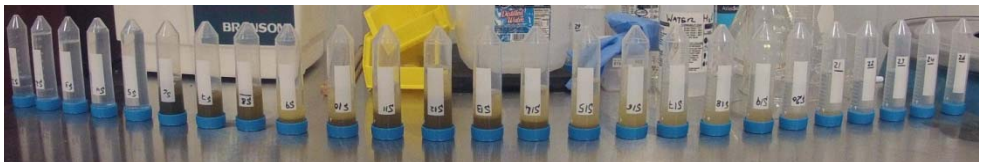

Fig. 3: Samples collected through the acidizing of core CTS-16.

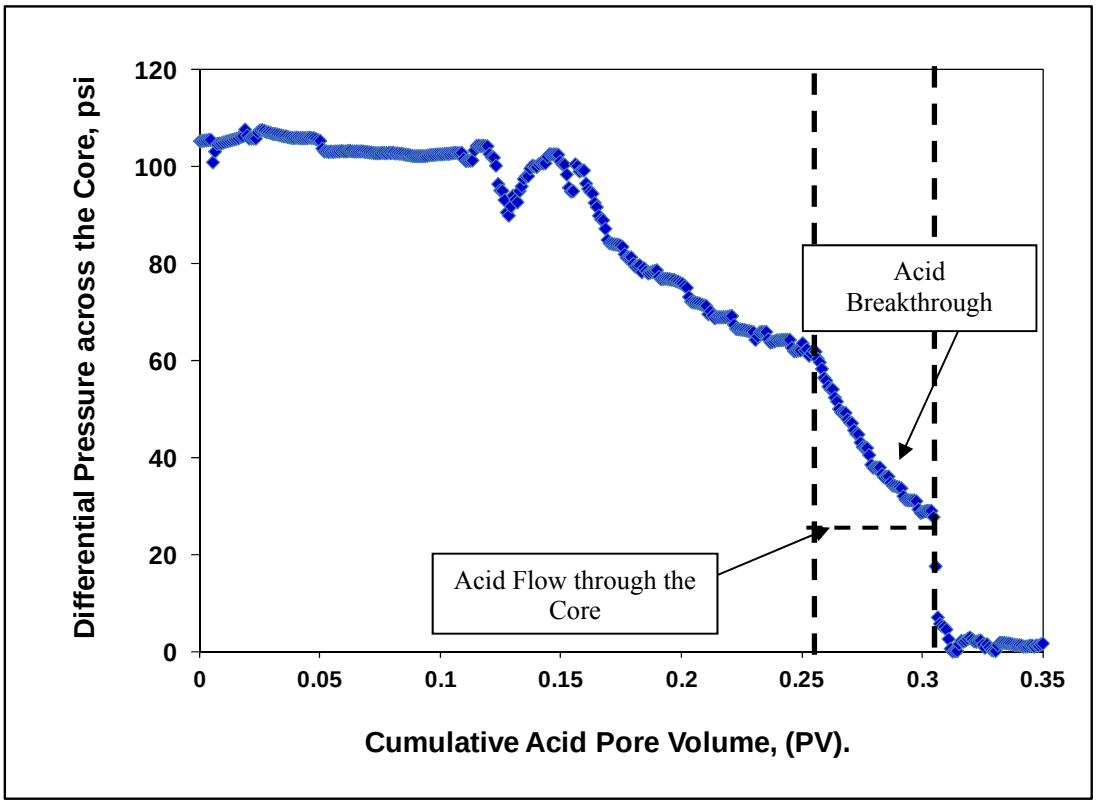

Fig. 4: Differential pressure across CTS-20 as a function of cumulative acid pore volume.

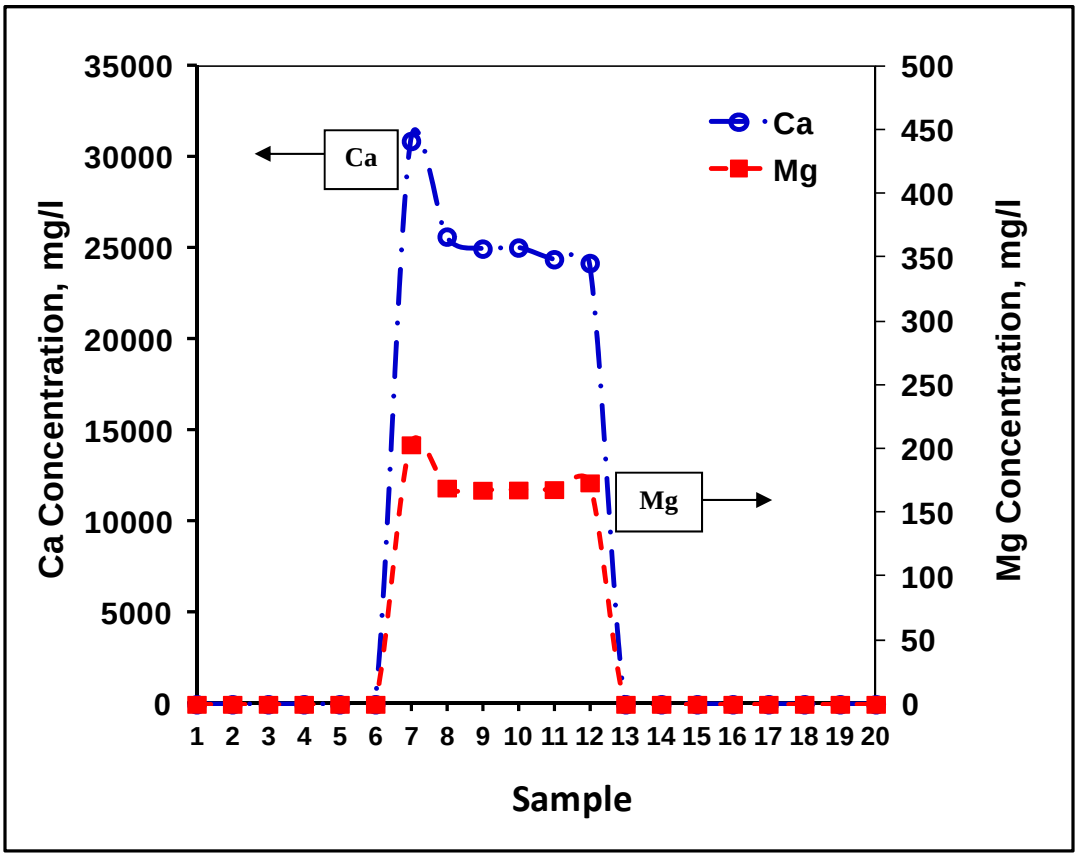

Fig. 5: Ca and Mg concentration in the effluent samples during acidizing core CTS-20.

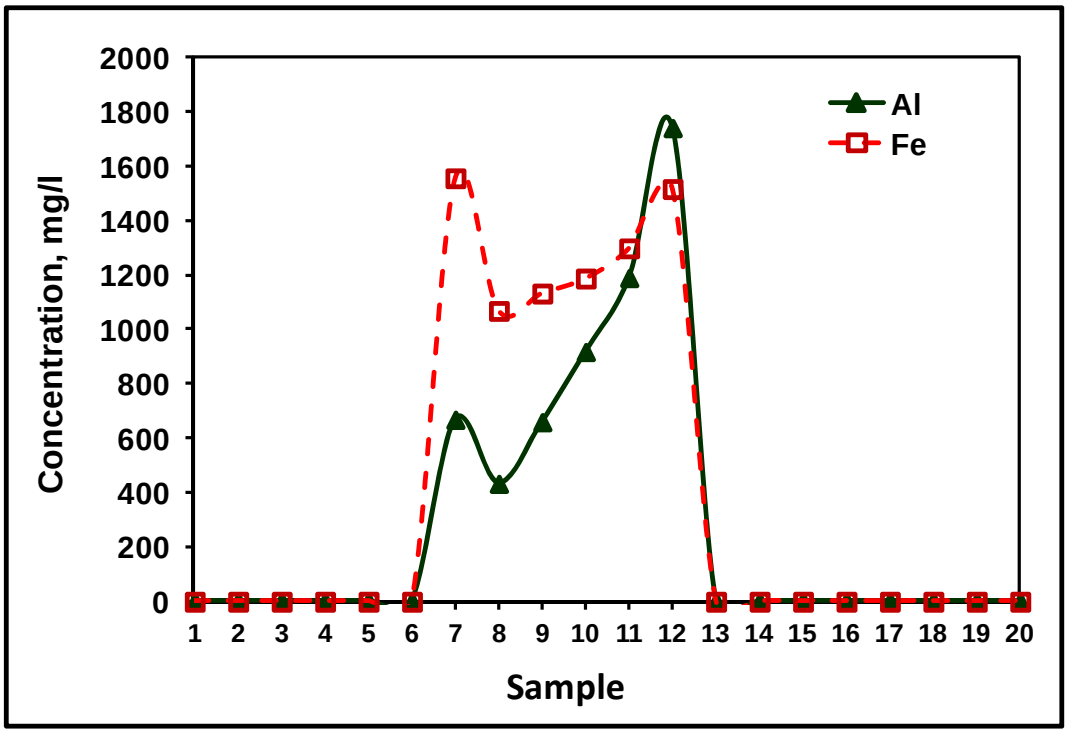

Fig. 6: Al and Fe concentration in the effluent samples during acidizing core CTS-20.

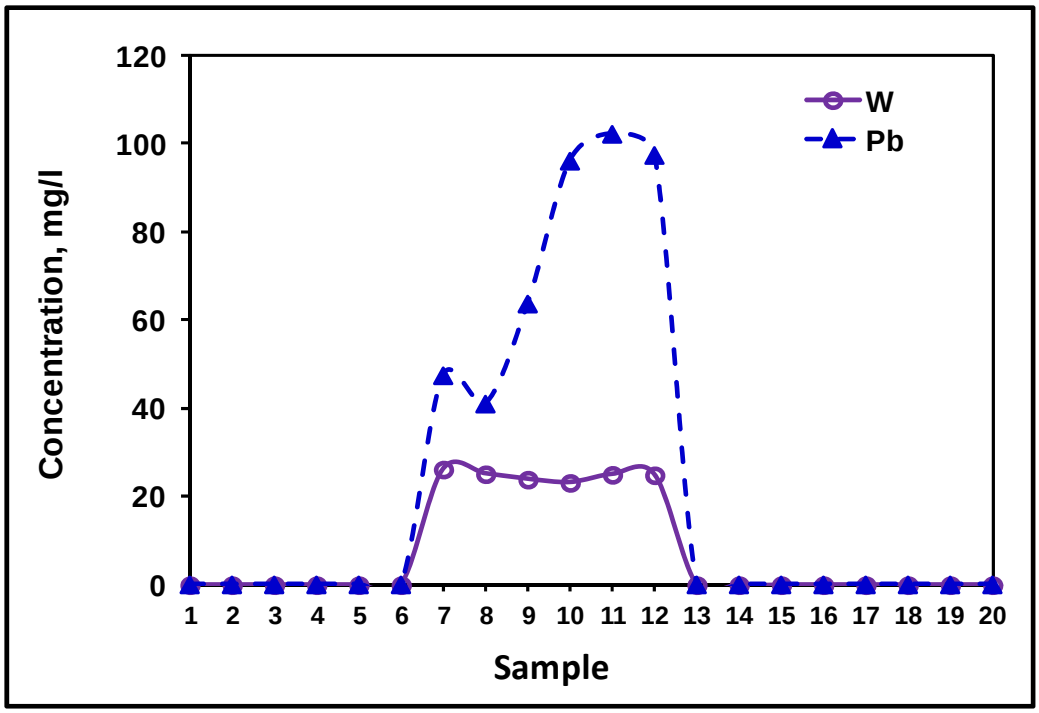

Fig. 7: W and Pb concentration in the effluent samples during acidizing core CTS-20.

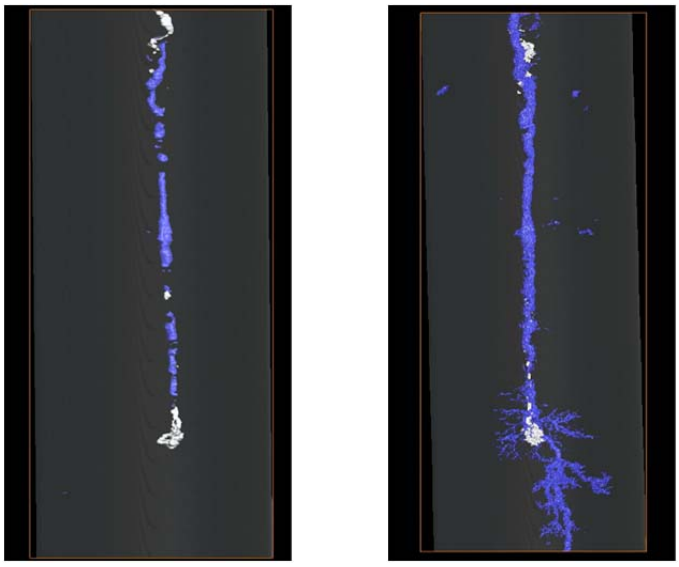

a) Before Acidizing b) After Acidizing

Fig. 8: Longitudinal section of CT-images of core CTS-20 (Reactive GH) before and after acidizing.

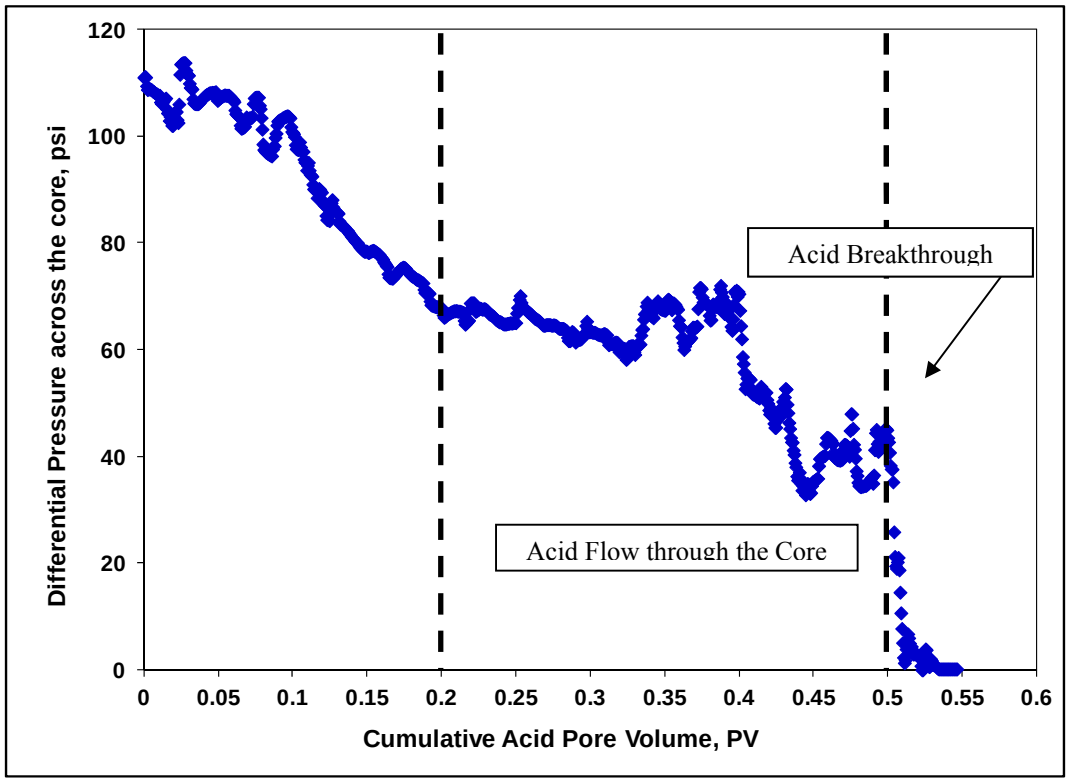

Fig. 9: Differential pressure across CTS-11as a function of cumulative acid pore volume.

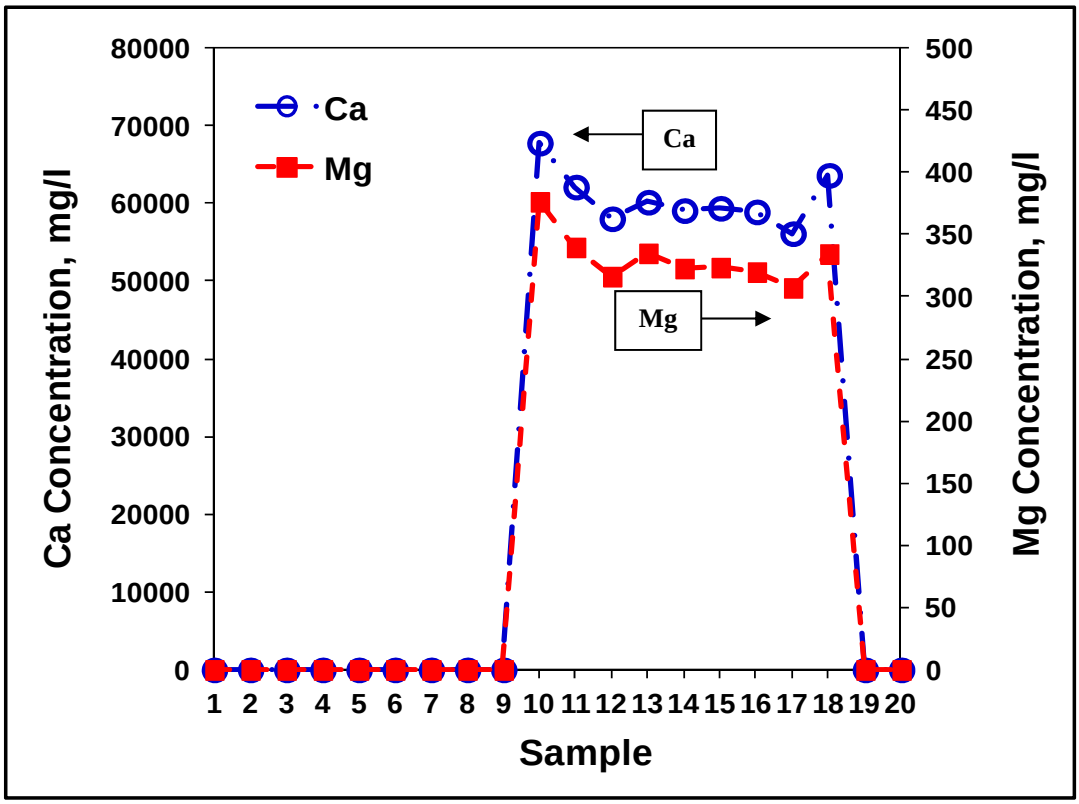

Fig. 10: Ca and Mg concentration in the effluent samples during acidizing core CTS-11.

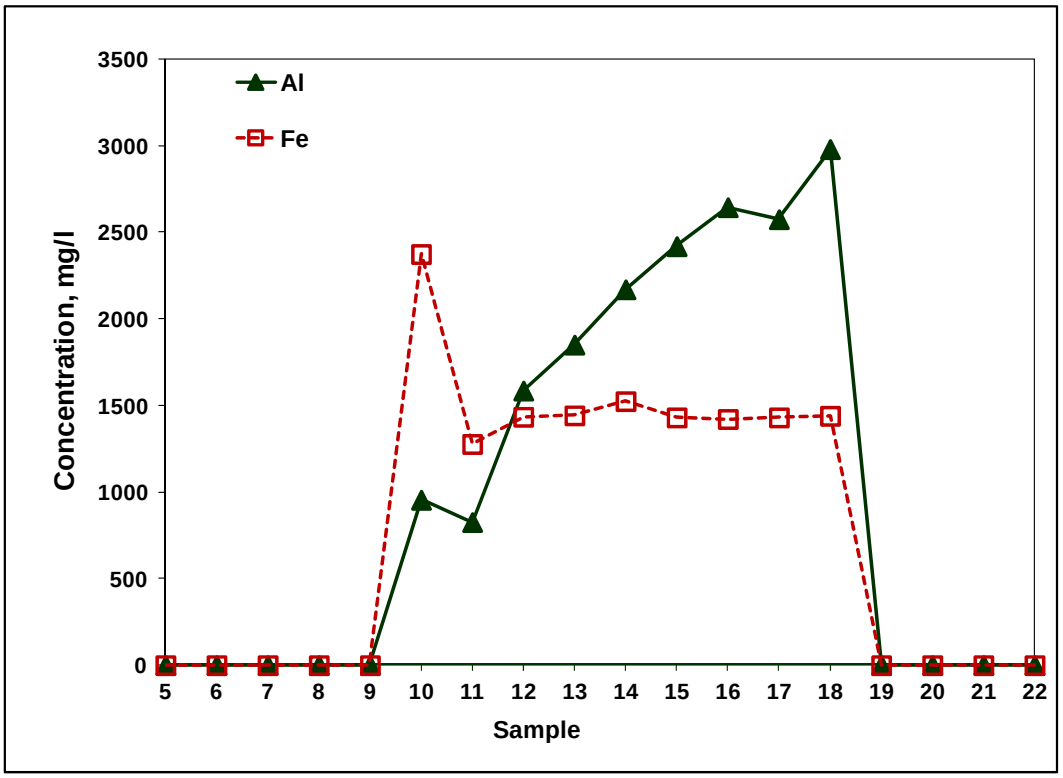

Fig. 11: Al and Fe concentration in the effluent samples during acidizing core CTS-11.

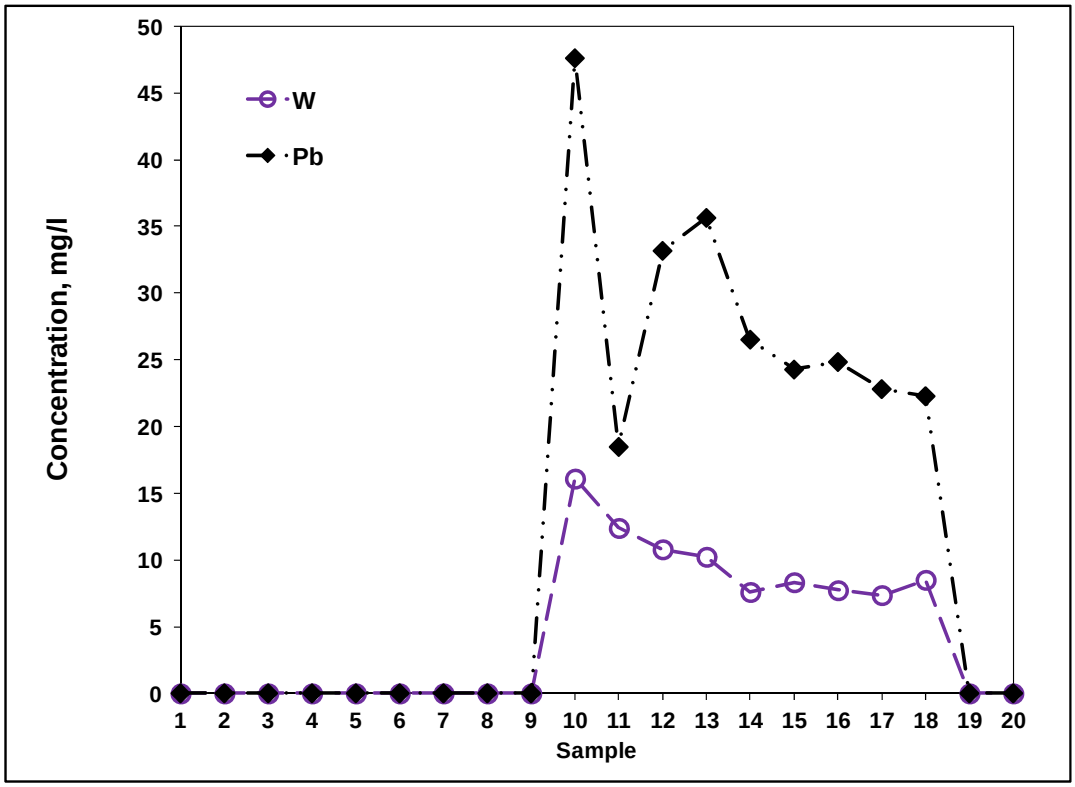

Fig. 12: W and Pb concentration in the effluent samples during acidizing core CTS-11.

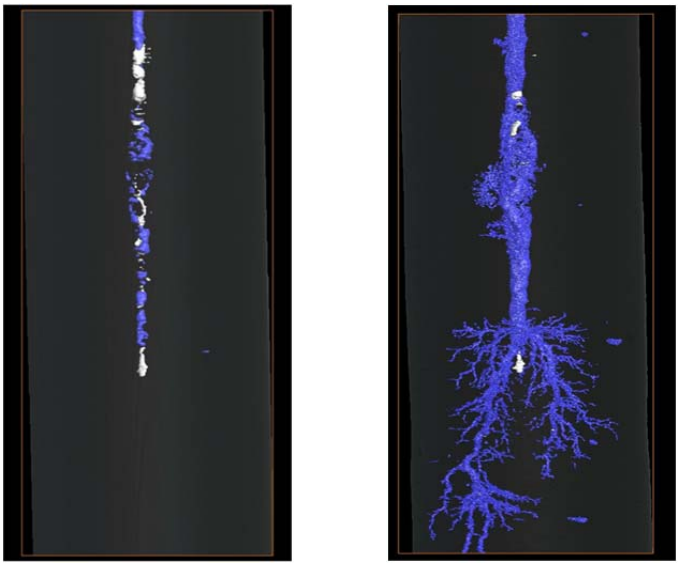

a) Before Acidizing b) After Acidizing

Fig. 13: Longitudinal sectional CT-images of core CTS-11 (Conventional GH) before and after acidizing.

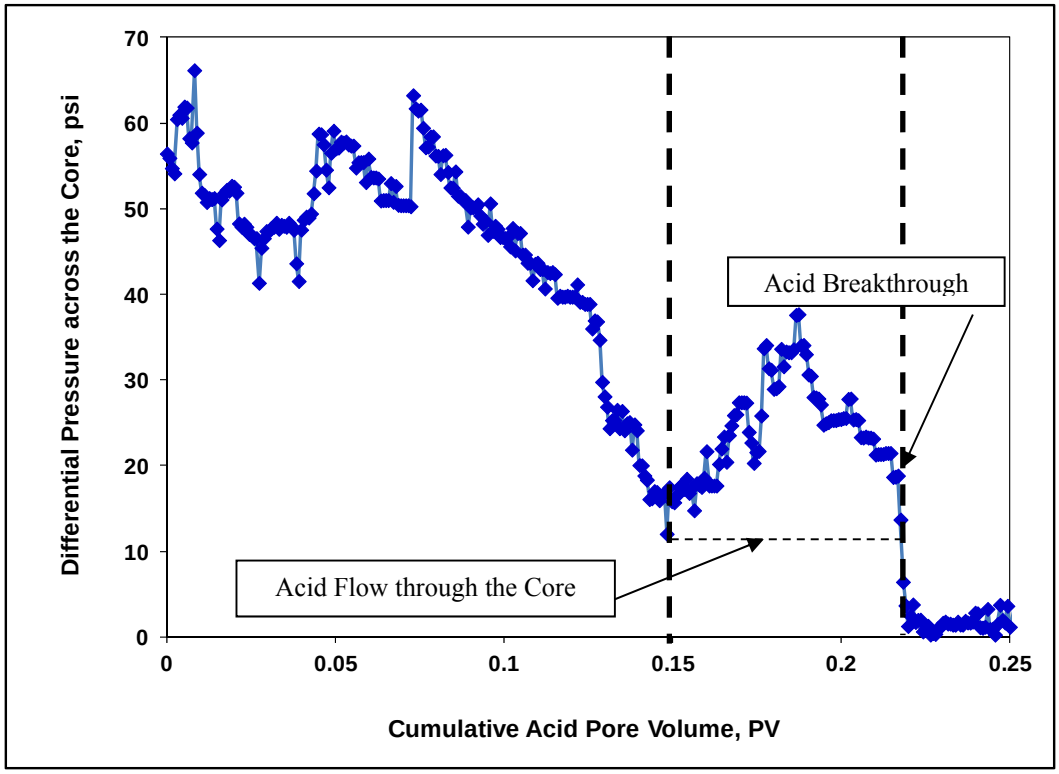

Fig. 14: Differential pressure across CTS-15 as a function of cumulative acid pore volume.

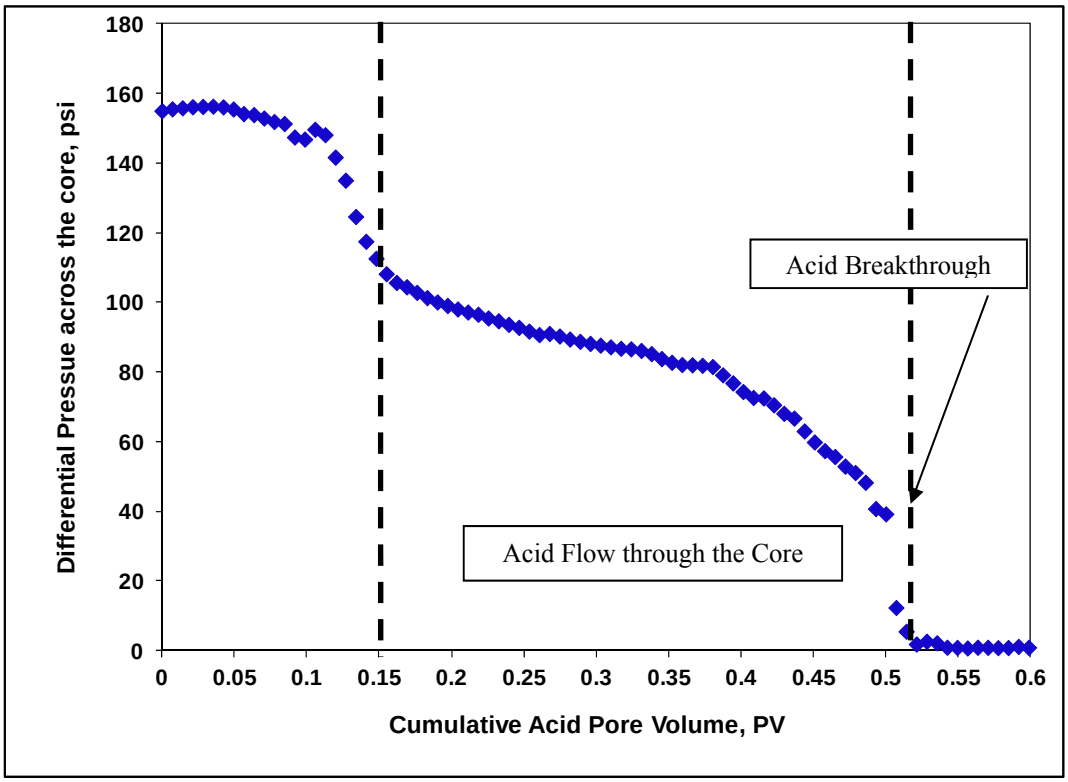

Fig. 15: Differential pressure across CTS-09 as a function of cumulative acid pore volume.

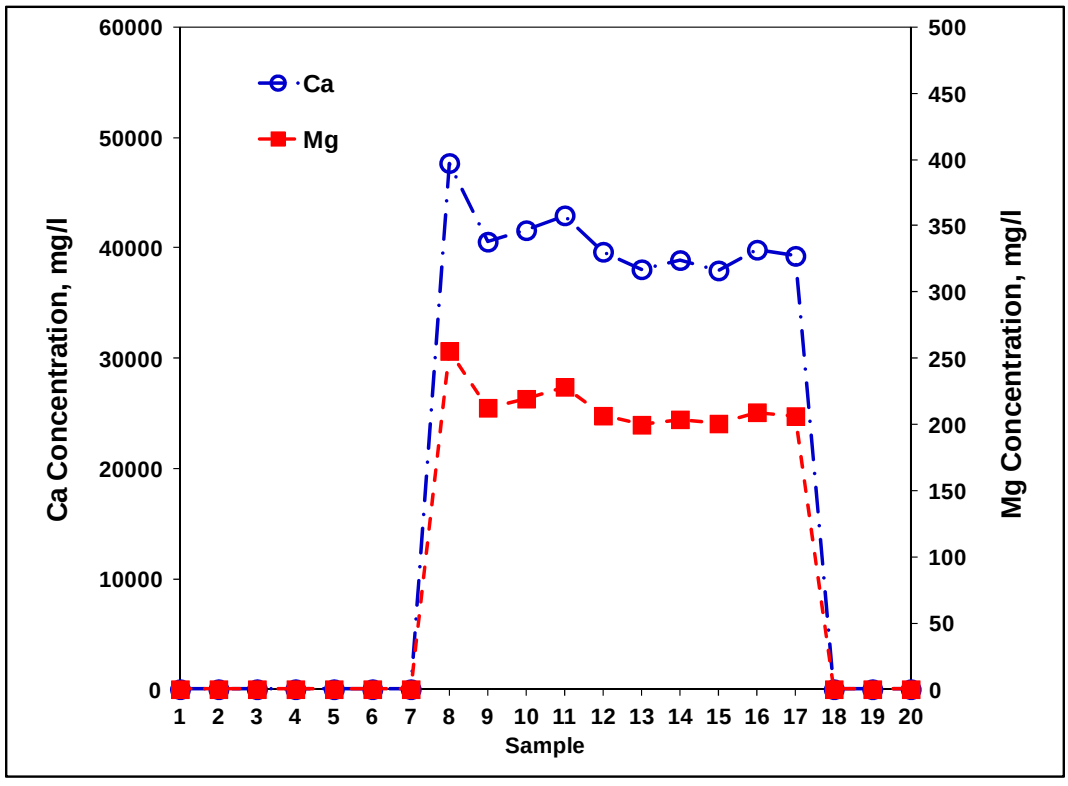

Fig. 16: Ca and Mg concentration in the effluent samples during acidizing core CTS-15.

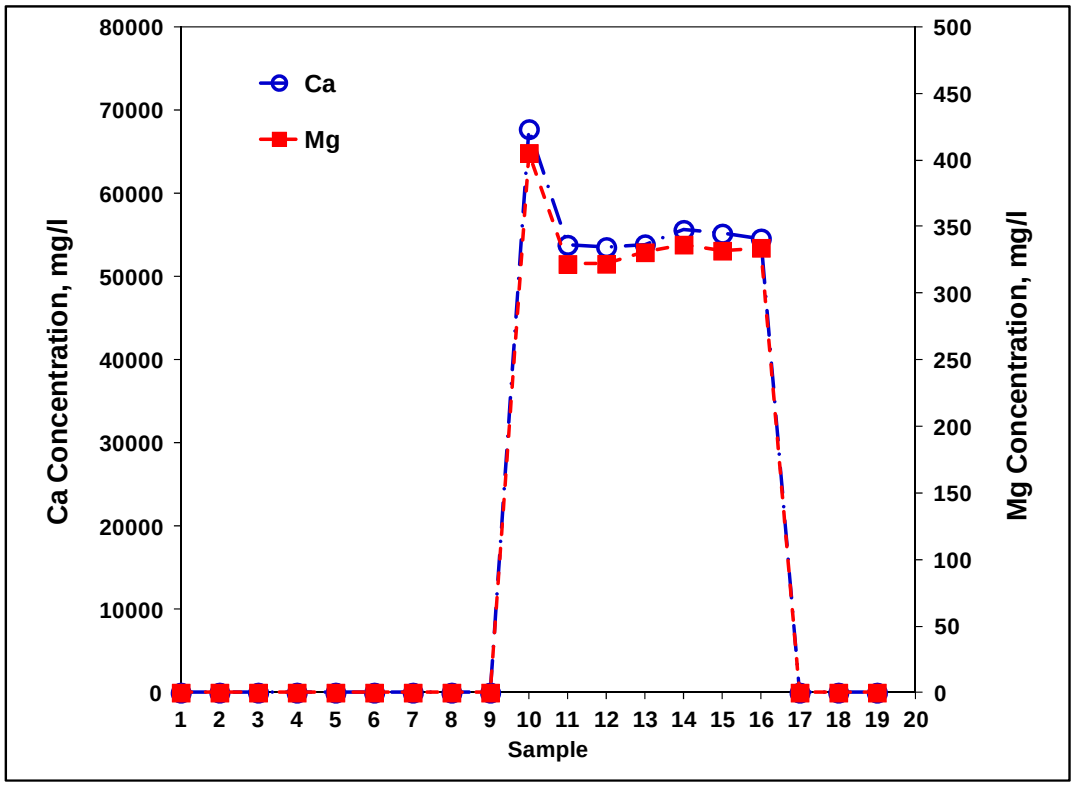

Fig. 17: Ca and Mg concentration in the effluent samples during acidizing core CTS-09.

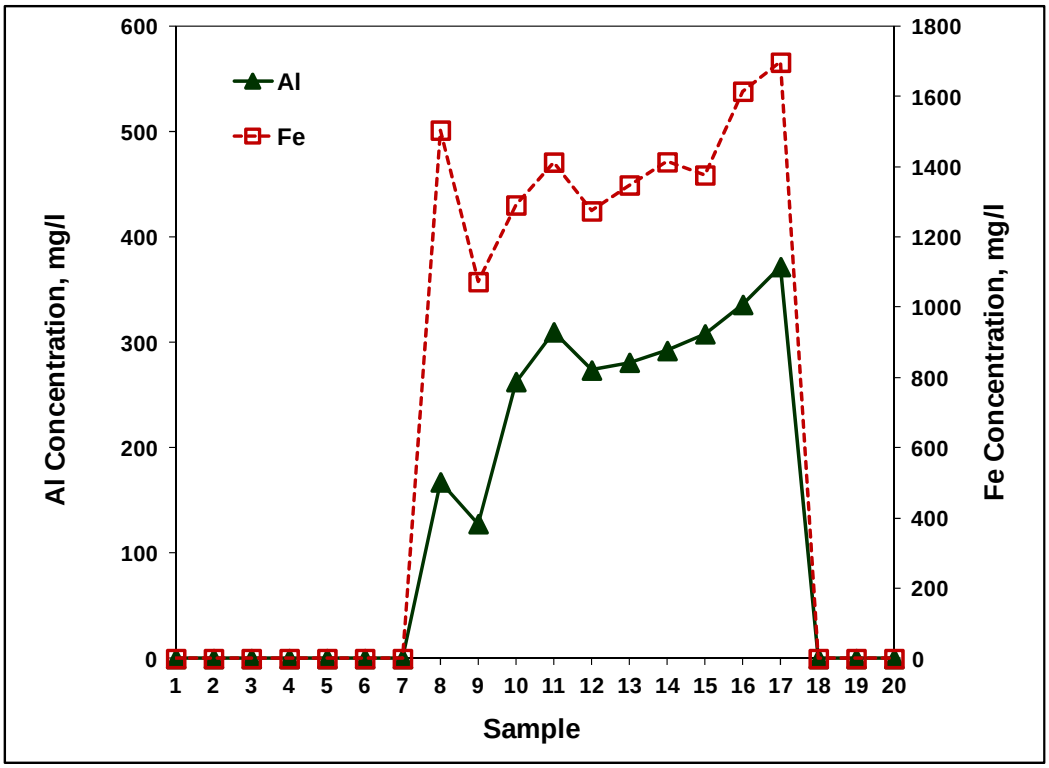

Fig. 18: Al and Fe concentration in the effluent samples during acidizing core CTS-15.

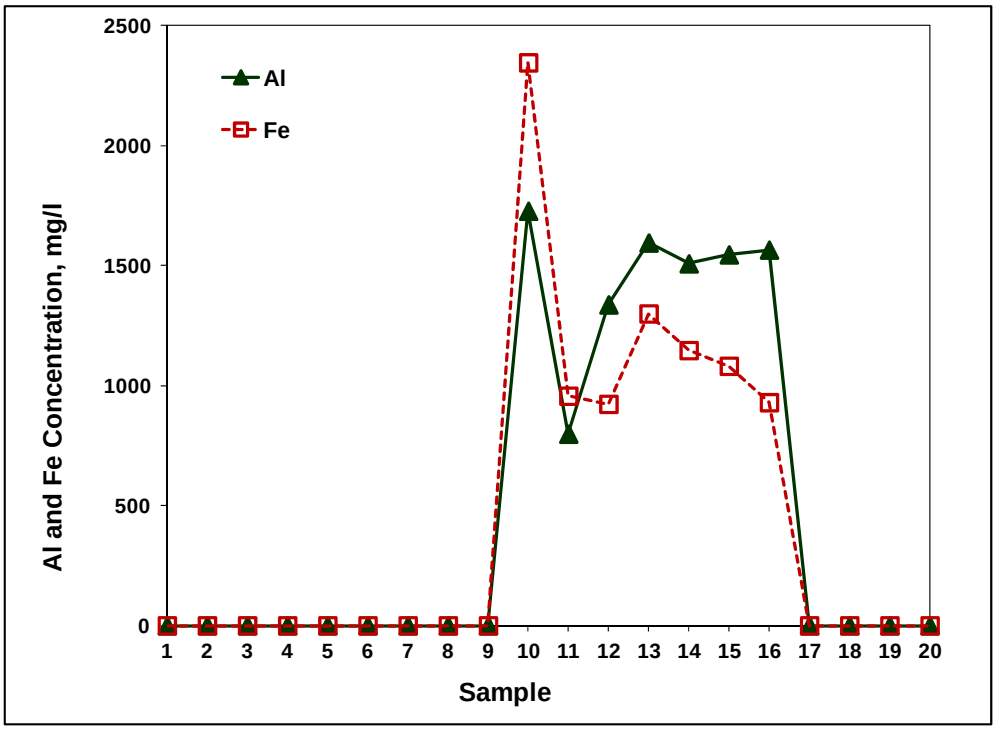

Fig. 19: Al and Fe concentration in the effluent samples during acidizing core CTS-09.

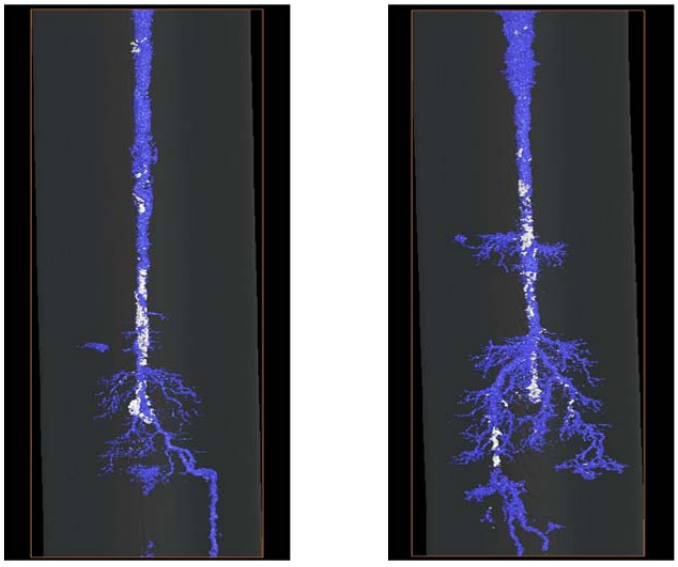

a) CTS-15 (Reactive Charge) b) CTS-09 (Conventional Charge)

Fig. 20: Longitudinal sectional CT-images of cores CTS-09 and CTS-15 (23g DP) after acidizing.

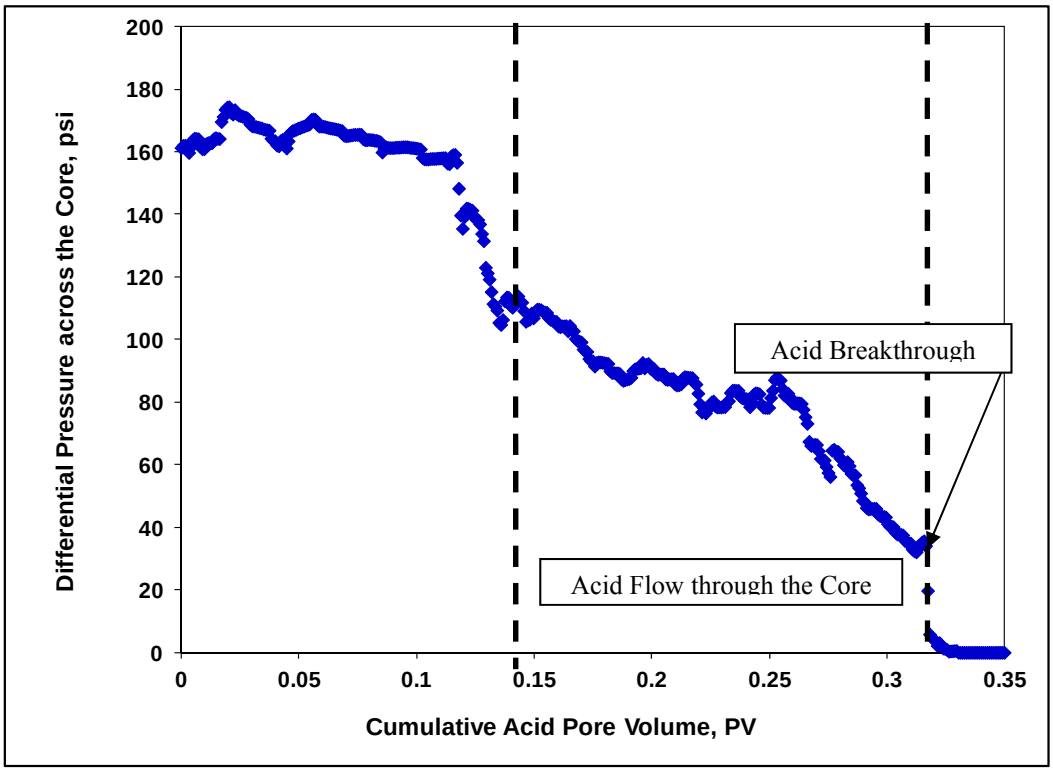

Fig. 21: Differential pressure across CTS-22 as a function of cumulative acid pore volume.

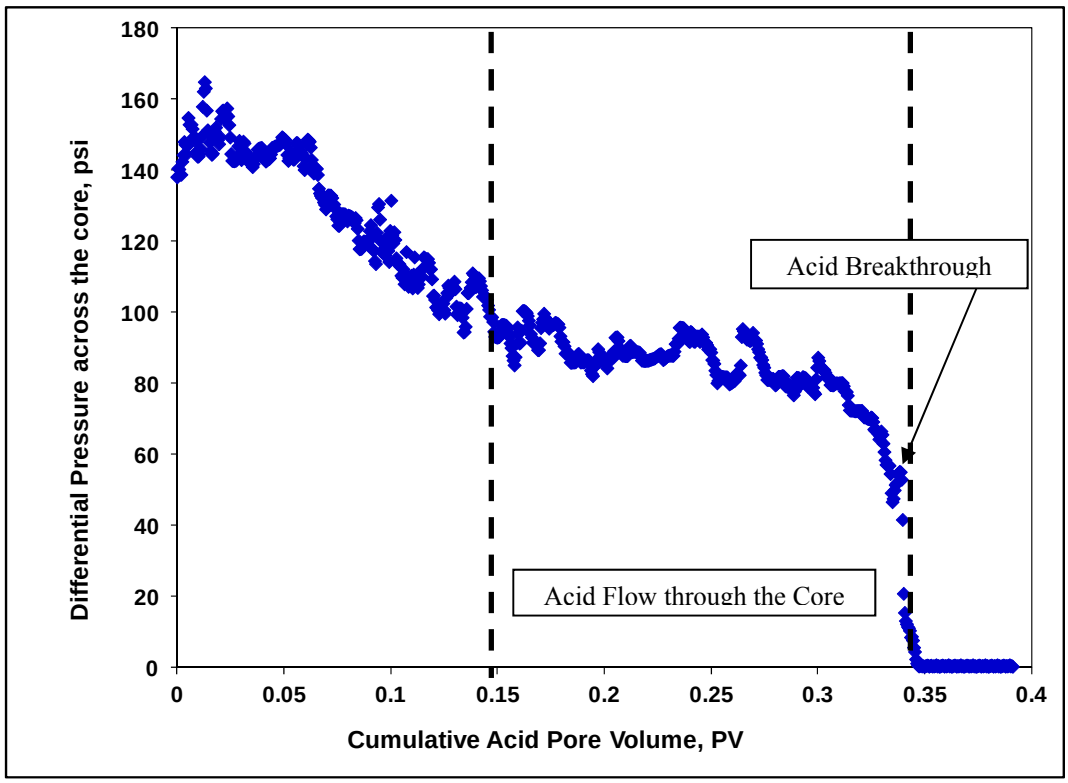

Fig. 22: Differential pressure across CTS-16 as a function of cumulative acid pore volume.

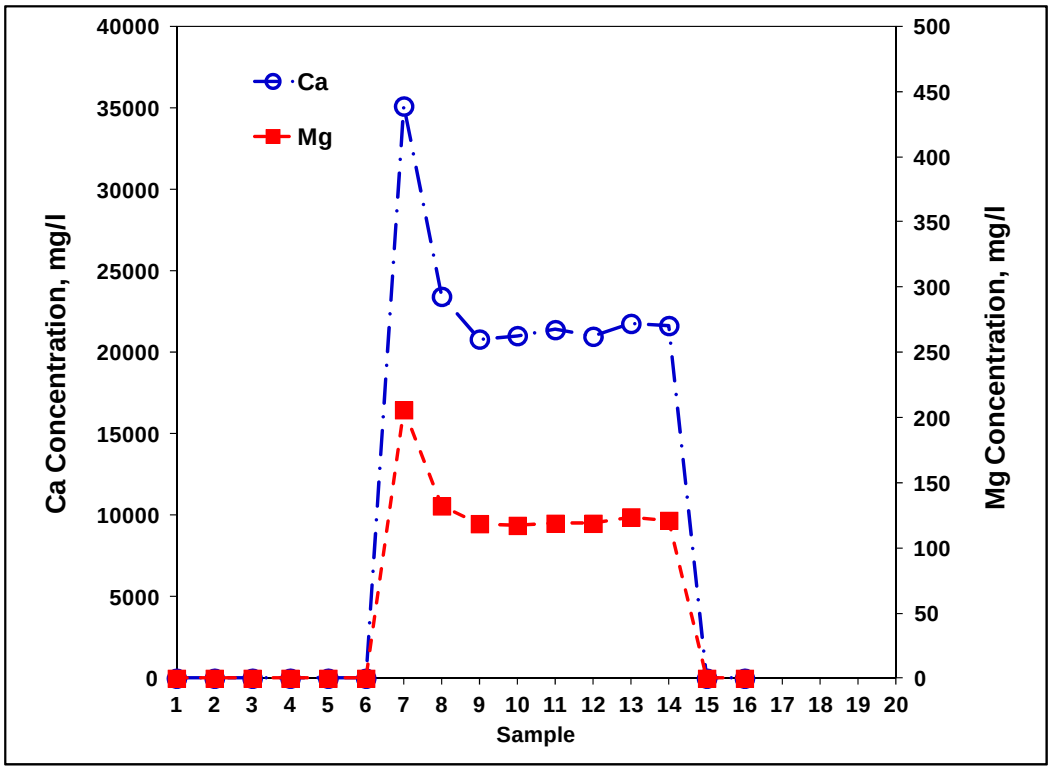

Fig. 23: Ca and Mg concentration in the effluent samples during acidizing core CTS-22.

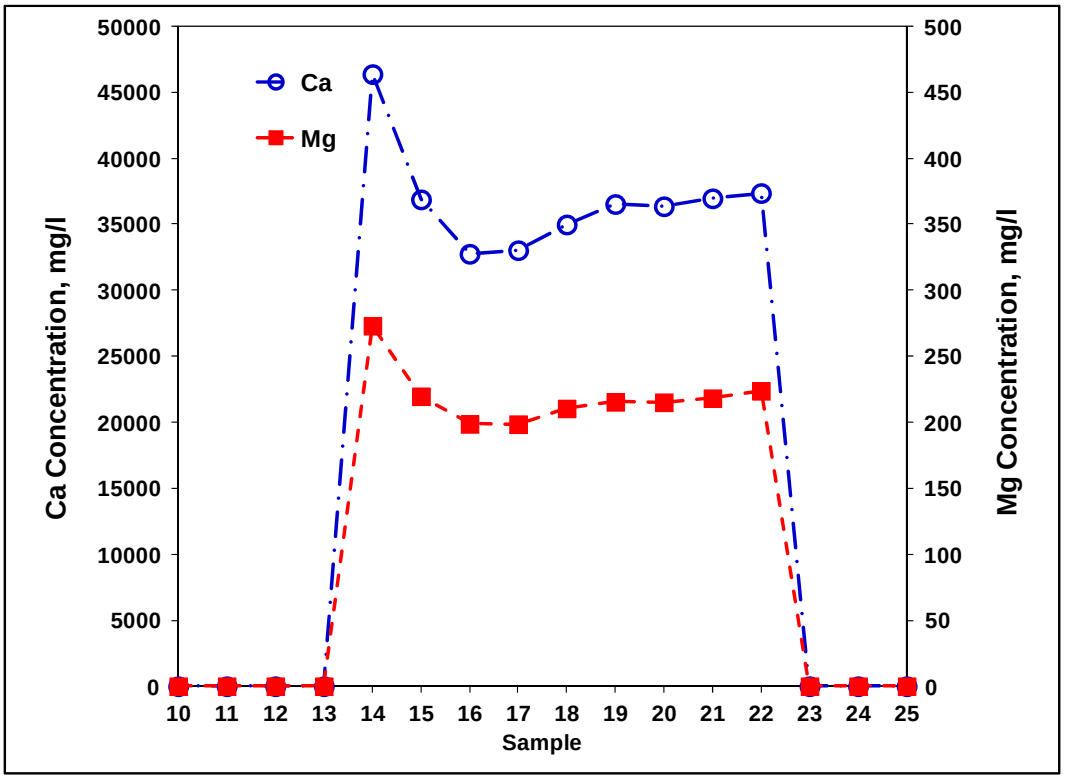

Fig. 24: Ca and Mg concentration in the effluent samples during acidizing core CTS-16.

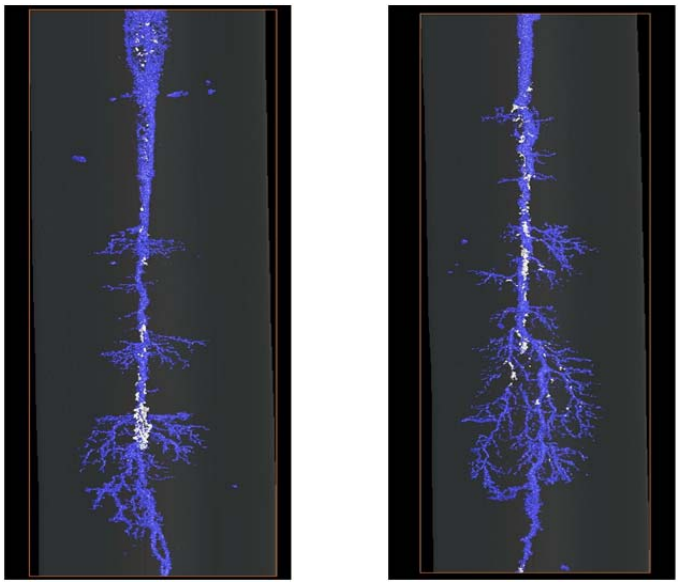

a) CTS-22 (Reactive Charge) b) CTS-16 (Conventional Charge)

Fig. 25: Longitudinal sectional CT-images of cores CTS-22 and CTS-16 (15g DP) after acidizing.

SPE 138434

An Evaluation of the Impact of Reactive Perforating Charges on Acid Wormholing in Carbonates

N.J. Diaz, Texas A&M University, M.R.G. Bell, J.T. Hardesty, Geodynamics, Inc. A.D. Hill, H.A. Nasr-El-Din, Texas A&M University, All SPE

This paper was prepared for presentation at the SPE Latin American & Caribbean Petroleum Engineering Conference held in Lima, Peru, 1–3 December 2010.

Abstract

The introduction of reactive perforating systems has led to tremendous improvements in well stimulation and productivity. Reactive charges generate a secondary energy release in the perforation tunnel immediately after it is formed, breaking up and expelling debris to leave clean tunnels across the perforated interval, irrespective of formation properties.

Although Bartko et al. (2007) have shown that clean perforation tunnels facilitate the evolution of a single, deeper-penetrating wormhole, there are no reported applications of reactive shaped charges in carbonates prior to acid stimulation. The present study was instigated to evaluate the impact of reactive charges on acid wormholing in representative carbonate cores.

A set of oil-saturated cores have been perforated under simulated downhole conditions, using either a conventional or a reactive shaped charge of equal explosive load. After CT scanning to eliminate outlying perforations affected by rock property anomalies, the set of cores were subjected to identical acid injection treatments representative of typical carbonate reservoir stimulations. Time to breakthrough and effluent chemistry were both analyzed and recorded. Finally, post-stimulation CT scans were used to evaluate wormhole morphology.

The laboratory experiments showed that reactive charges provide cleaner perforation tunnels with higher injectivity, which is beneficial for any type of stimulation job. Higher injectivity tunnels help to propagate more dominant and straighter wormholes resulting in less acid to propagate a given distance. This technology has a significant potential when perforating tight formations or heterogeneous intervals, where obtaining clean tunnels with conventional perforators is most challenging. Further research work needs to be done to evaluate if the difference in acid volume to breakthrough observed in the experiments would have a major impact in the field.

Introduction

Perforation tunnels are the communication path between the wellbore and the reservoir in cased-hole completions. Thus the main objectives of perforating shaped charges are to by-pass formation damage and enhance well productivity, which is achieved by maximizing penetration length and minimizing perforation damage.

Some perforating techniques have been developed to enhance well productivity, such as static under balanced and dynamic underbalanced perforating. These two techniques rely on the underbalanced condition achieved during the initiation of the perforation. The difference between these two techniques is that the dynamic underbalanced technique is designed to allow the high pressure wellbore and reservoir fluids flow into the empty guns and tubing, and the static underbalanced method does not. Therefore, the wellbore pressure goes from underbalanced to balanced much faster when perforating using the static underbalanced technique. Moreover, the dynamic underbalanced can be achieved regardless of the initial static condition. The objective of these techniques is to clean up perforation tunnels and improve their performance, by expelling the liner debris and crushed rock. But the main limitation of these techniques is that the flow needed to clean the perforation tunnels may not be achieved in tight formations.

Obtaining deep and clean perforations may still not be enough to provide the desired production rate. Therefore, a common practice is to carry out a matrix acidizing treatment in carbonate formations after completion, to create high permeability channels

called wormholes It is believed that acid partially dissolves perforation debris while creating wormholes and can overcome perforation and near wellbore damage, thus the tunnels' shape and perforation damage are often not considered important for the acidizing treatment. On the other hand, Bartko et al. (2007) presented a research study in which the effect of perforation tunnels on matrix acidizing treatments is discussed, different perforating techniques were tested, and it was shown that perforating design plays an important role in creating a single and deep-penetrating wormhole, and in obtaining a smaller post-treatment skin factor. There have been many research studies regarding the parameters that need to be considered when designing a matrix acidizing treatment, such as; acid injection rate, temperature, rock properties, and acid additives. Few research projects have taken into consideration the perforation tunnels.

The main objective of this work is to study the impact of reactive shaped charges on acid wormholing in carbonate rocks. Bell et al. (2009) studied the performance of reactive shaped charges in sandstones, and it was demonstrated that this type of charge offers significant productivity improvement across a wide range of conditions.

The dynamic under balanced technique is not recommended for tight or low quality rock formations, because the under balanced pressure may not be enough to provide sufficient driving force to expel the debris from the tunnels due to the low formation permeability. But reactive charges generate a secondary reaction in the perforation tunnels, which expels the debris to leave clean and undamaged tunnels even in tight or low quality rock formations, independently from the pressure difference condition.

The purpose of this research is to test the performance of both reactive and conventional charges and evaluate their effects on the matrix acidizing process. This was accomplished by comparing the flow performance of the perforated cores, by examining CT scans before and after acidizing, by comparing the acid volume to breakthrough for each type charge, and by comparing wormhole geometries.

Background

Since the introduction of perforating technology in 1932, perforations' effectiveness has been based on well productivity. Shaped charges' goal is to enhance well productivity by creating long perforations to by-pass the casing, cement and the contaminated zone resulting from drilling operations. It is known that the stress created by the action of the jet penetrating the rock forms a damaged zone around the perforation tunnel that is commonly called "the crushed zone". This fact has led to studies aimed at improving tunnel performance by trying to expel liner debris and crushed rock around the perforation tunnels.

It is vital to obtain clean perforation tunnels in order to achieve the desired well productivity, and a standard practice currently applied to clean perforation tunnels is the dynamic underbalanced technique, the effectiveness of which depends on the near wellbore formation permeability. The limitation of this technique is the driving force required to clean the tunnels may not be achieved in tight or low quality rock formations.

Obtaining clean tunnels may still not be enough to generate the required well productivity due to the formation characteristics, thus a matrix acidizing treatment is commonly carried out. Even though stimulation may be needed after perforating, the cleaning of the tunnels has significant importance at the moment of designing an acidizing job, because clean tunnels can provide higher injectivity which would lower the injection pressure needed at the surface, and would also help in obtaining single and deep penetrating wormholes.

The purpose of this research is to study the impact of reactive shaped charges on carbonate wormholing. The type of shaped charge tested in this research generates a secondary reaction in the perforation tunnel caused by the liner metallurgy properties and charge design. The reaction drives the expulsion of liner debris and crushed zone materials, leaving a clean and undamaged tunnel. The reactive charge can be detonated in conventional gun hardware, without requiring any special handling, storage, loading or running procedures. Shot density and phasing can be the same as conventional charges. Once the explosive detonates, it converts the conical shaped charge liner into a fast-moving jet of particles, which is able to pass through the gun body, casing, cement and formation in the same way as conventional charges. Then the liner materials deposited in the perforation tunnels react exothermically, generating heat and pressure within the perforation tunnel. The overpressure breaks up and expels crushed zone materials and debris.

Experimental Procedure

This research work is based on seventeen core flood experiments, eleven of which were carried out with Indiana limestone cores and six with cream chalk cores. In order to compare the results obtained from the experiments, the cores were cut from the same block of rock, which provides the certainty that the rocks have similar properties.

After selecting the type of rock and cutting the core samples, they are saturated by placing the cores in a container connected to a vacuum pump. The vacuum pump is used to force the liquid to go into the pore space. Mineral oil was used for saturation and to run the experiments. Once the cores are saturated, the weight of the wet rocks is measured so that the pore volume and porosity of the core can be calculated. **Fig. 1** shows picture photograph of one Indiana limestone core sample (right side) and one cream chalk core sample (left side), which are 20 inches long and 4 inches in diameter.

Fig. 1—Carbonate core samples

The cores are then loaded into the pressure vessel to carry out the perforating (**Fig. 2**). The coreholder is filled with fluid, and then the pore pressure is applied at the same time the overburden pressure is applied. Once the desired wellbore and pore pressure are reached, the charge is detonated. Later the wellbore and pore pressure are allowed to equalize, and the overburden pressure is slowly reduced at the same rate that the pore pressure is released. When the wellbore and pore pressure reach atmospheric pressure, the coreholder is opened to retrieve the gun.

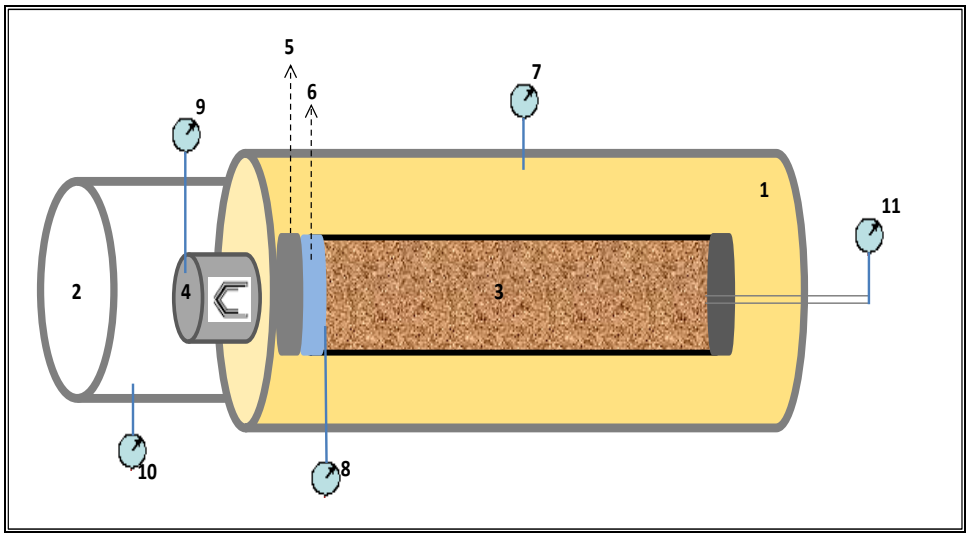

Fig. 2—Perforating set-up. (1) Confining chamber (2) Simulated wellbore (3) Core sample (4) Gun with shaped charge (5) Simulated casing (6) Simulated cement (7) Pressure transducer (8) Pressure transducer for core inlet pressure (9) Pressure transducer for gun pressure (10) Pressure transducer for wellbore pressure (11) Pressure transducer for reservoir pressure.

After perforating the core samples, they are characterized by using CT scanning. This step is carried out to identify geometric anomalies and fracturing caused by variations in the rock targets, and also to evaluate the original condition of the perforation

tunnels. The images of the scans are generated from a set of CT numbers, which correspond to the density of the materials scanned. High CT numbers represent materials with high density and small CT numbers represent materials with low density. Thus the length and diameter of the perforation tunnels can be obtained from the images, since the range of CT numbers in the perforation tunnel zone is different from the range of CT numbers of the rock. The presence of debris can be identified as well, since the range of CT numbers of the rock is different from the range of CT numbers of the liner materials.

The CT scanner is set to take a picture of the core every 3 mm. **Fig. 3** shows an example of a perforated core image. It can be observed on this picture that there are different colors in the core sample. The color green represents the matrix, the color blue represents the perforation tunnel free of debris, and the pink or red color represents the debris inside the perforation tunnel. At the bottom of the figure there is a legend, which indicates the CT number rage for every color.

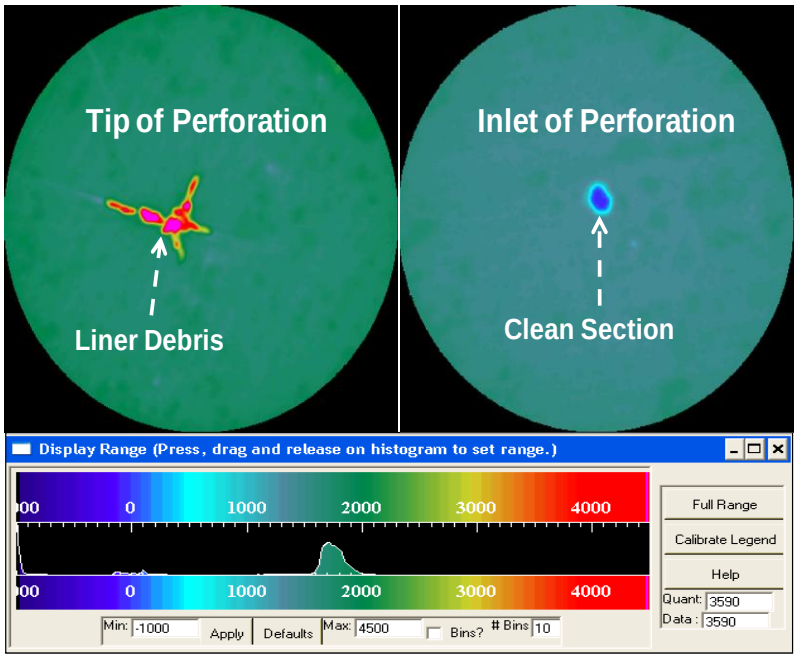

Fig. 3—2D CT images of perforated cores.

Every slice can be studied independently to identify the presence of debris and measure the dimensions of the perforation tunnel at any part of the core. This set of slices is then converted into a three dimensional picture, which is shown in **Fig. 4**. The three dimensional image is used to identify the flow path of acid and observe the wormholes.

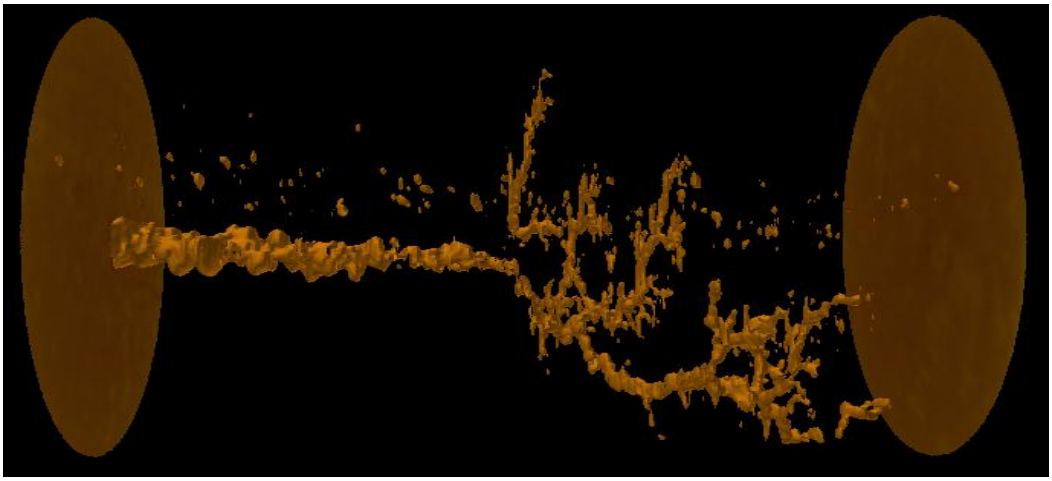

Fig. 4—3D CT image of entire core sample.

The cores are then placed in the core holder to perform the acid injection. The outlet pressure is set to 1000 psi to ensure that the pressure in the entire system is above 1000 psi, in order to keep the CO_2 that results from the reaction between HCL and $CaCO_3$ in solution while acid is injected.

Once the apparatus is set, the flow performance of the core is evaluated by pumping mineral oil through the core sample at a 10 cm^3 /min rate, until steady state flow is reached. This step is carried out to compare the flow performance of the cores perforated with conventional and reactive shaped charges before acidizing. Since the core samples have similar properties, the flow performance of the cores is affected just by the efficiency of the perforation tunnels. The pressure is recorded while running the entire experiment, this allows the monitoring of the pressure in real time. The injectivity of the core sample is measured and the results are shown and analyzed in the following section. **Fig. 5** shows a typical pressure response during a core flood experiment, from which can be observed that steady state flow is reached at 368 psi pressure difference.

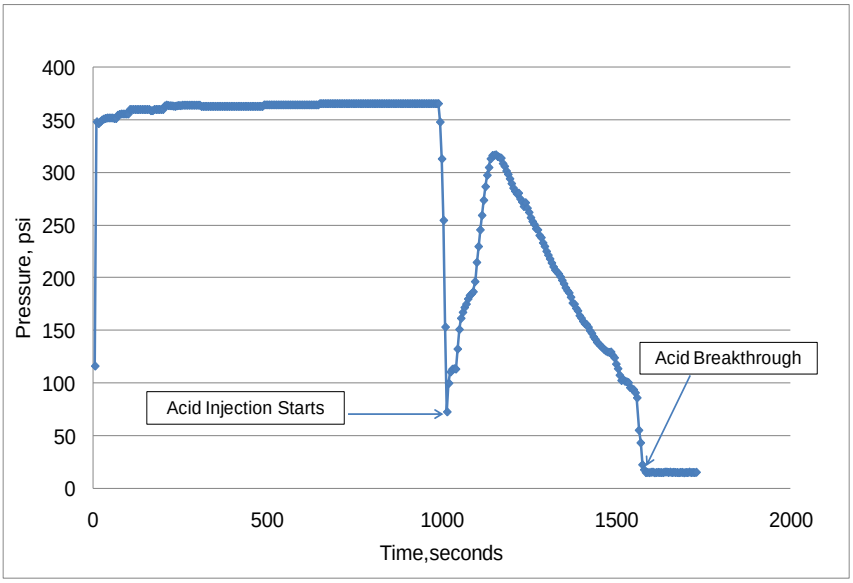

Fig. 5—Typical pressure response during a core flood experiment.

After reaching steady state flow, there is a pressure decline due to the switch from oil to acid (the pump has to be stopped to close and open some valves). Later pressure starts increasing as acid is injected, a peak is reached and then pressure decreases as the acid reacts with the rock and wormholes propagate until acid breaks through the core. Acid volume to breakthrough is measured to later calculate the pore volumes needed to breakthrough, this is done by calculating the pore volume from the tip of the perforation to the end of the core, which is the area that acid has to flow through. The pore volume needed to breakthrough is just the ratio of acid volume divided by the core pore volume.

After acidizing, a flow back is carried out by pumping oil in the opposite direction. This step is carried out to simulate a real stimulation treatment in the field. This allows identification of the presence of liner debris remaining in the perforation tunnel after acidizing. If liner debris remain in the perforation tunnel after acidizing, some of it would be observed coming out from the flow lines.

Fluid samples are collected throughout the core flood experiment. This step is carried out to perform a compositional analysis of the effluent by measuring the acid and calcium concentrations. The acid (HCL) concentration is measured with the acid base titration method by using an autotitrator, and the calcium concentration is measured with an atomic absorption spectrometer. Since there is not an accurate technique to calculate the amount of debris from the CT scan images, the measurement of heavy metals concentration in the fluid samples could provide a better understanding of the cleaning efficiency.

Results and Discussion

As mentioned before, this research project is based on seventeen experiments, but due to the fracturing of some core samples, just six experiments are reported and analyzed in detail. The first set of core samples were Indiana limestone, and they were perforated using 15 gram charges. Long fractures were created due to the stress generated by the charge penetrating the rock. It was decided to run the core flood experiments with these cores, to determine whether these fractures would significantly affect the results or not. The fractures observed in these core samples trigger the collapse of the cores during the core flood experiments, and they highly affected the results (**Fig. 6**). The flow performance of the core samples was not dominated by the permeability of the core

itself and the perforation tunnels efficiency, the flow performance was highly affected by the fractures as well.

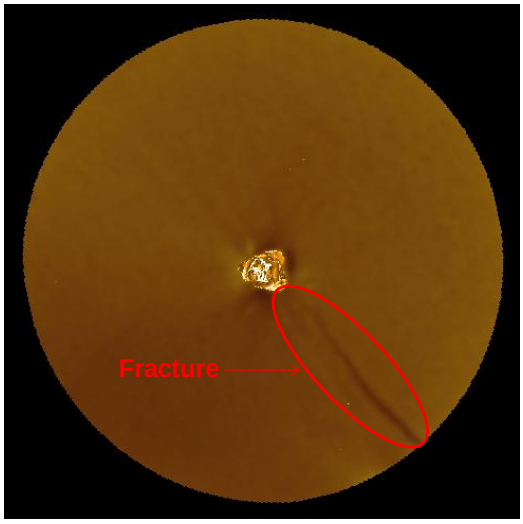

Fig. 6—Inlet face of a perforated Indiana limestone core sample.

The flow path of the acid (wormholes) was highly dominated by the fractures. Due to their high conductivity, acid flowed through the fractures as well as through the perforation tunnels (**Fig. 7**). Therefore, it was not possible to compare and evaluate the results obtained from these experiments. In order to try to avoid the fracturing of the cores, a second set of Indiana limestone cores were perforated with 7 gram charges rather than with 15 gram charges. Since this type of rock is highly brittle, these core samples were fractured as well during the shooting of the charges. The fractures significantly affected the results such as injectivity and volume of acid to breakthrough.

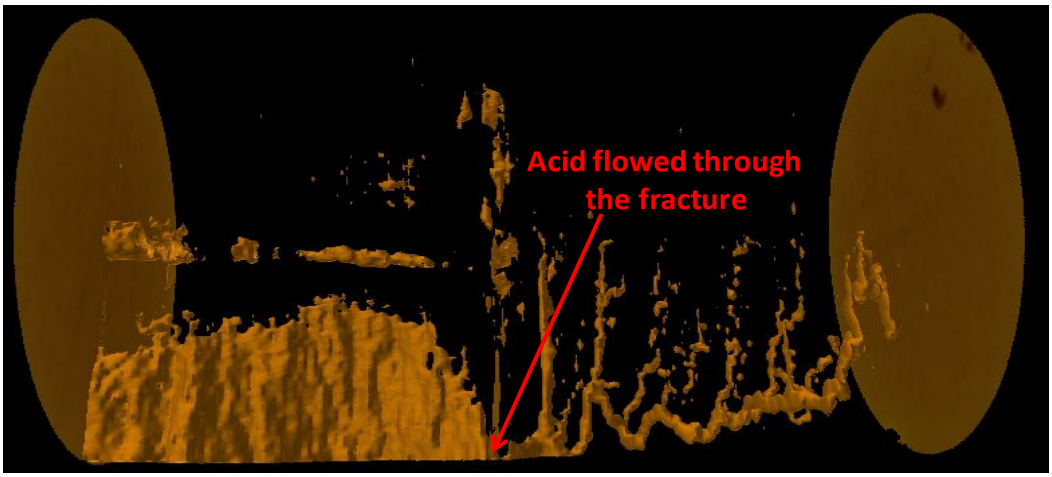

Fig. 7—3D Image of an Indiana limestone core sample after acidizing.

Since the fracturing of the cores was not allowing the comparison of the results, it was decided to perforate a set of cream chalk cores. This type of rock is softer than the Indiana limestone type, thus it was expected to avoid the fracturing of the core samples. The results obtained from the set of cream chalk core samples are the ones reported and analyzed in detail.

Six experiments were run using different charges and pressure conditions. **Table 1** summarizes the perforating results obtained. The first two samples of this set of cores were perforated at a balanced pressure condition, meaning that the pore pressure and simulated wellbore pressure were equal (3,000 psi) before the detonation of the 7 gram charges. **Fig. 8** shows the core perforated with a conventional charge (core 1) and **Fig. 9** shows the core perforated with a reactive charge (core 2). The presence of liner debris in both cores was observed, but there is not a method to accurately estimate the amount of debris from the CT scan images. Fractures were observed at the tip of the perforation tunnels in both cores, but the fractures are considerably longer in core 2. **Fig. 10** shows a comparison of the fractures at the tunnels' tip for cores 1 and 2. This observation confirms the fact that the

increase in pressure generated by the exothermic reaction propagates the length of these fractures, which are originally created by the liner penetrating the rock. The diameter of the perforation and the tunnel's length were observed to be larger in core 2, which resulted in a larger perforation tunnel volume. Since both shaped charges have exactly the same dimensions, this observation verifies that some of the crushed rock is expelled into the simulated wellbore.

Table 1—Perforating results

Test Number	Type of Shaped Charge	Perforating Pressure Condition	Inlet Perforation Diameter, inches	Perforation Length, inches	Volume of Perforation, cubic inches
Core 1	Conventional	Balanced	0.206	10.27	0.33
Core 2	Reactive	Balanced	0.257	10.39	0.49
Core 3	Conventional	Overbalanced	0.229	10.27	0.32
Core 4	Reactive	Overbalanced	0.263	10.51	0.50
Core 5	Conventional	Balanced	0.320	17.72	1.09
Core 6	Reactive	Balanced	0.390	15.42	1.05

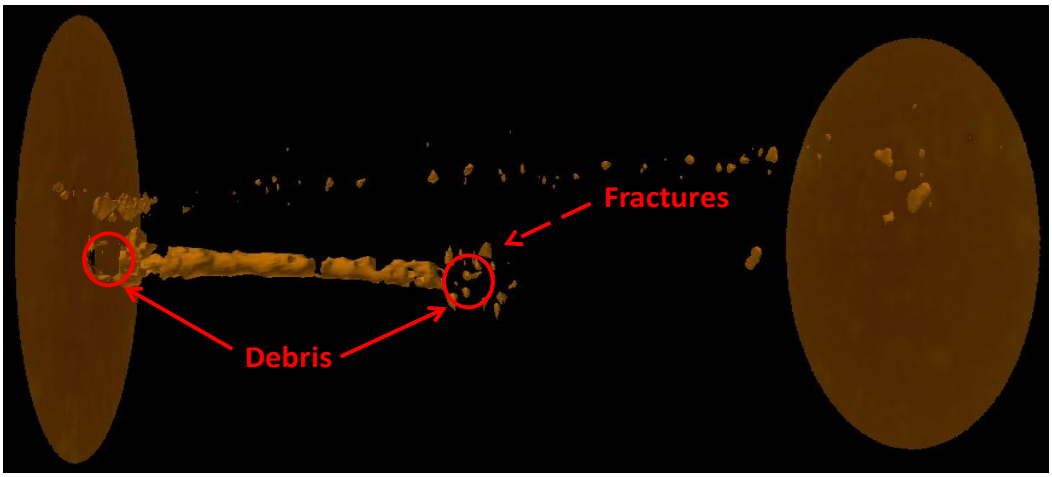

Fig. 8—3D Image of Core 1 – conventional charge.

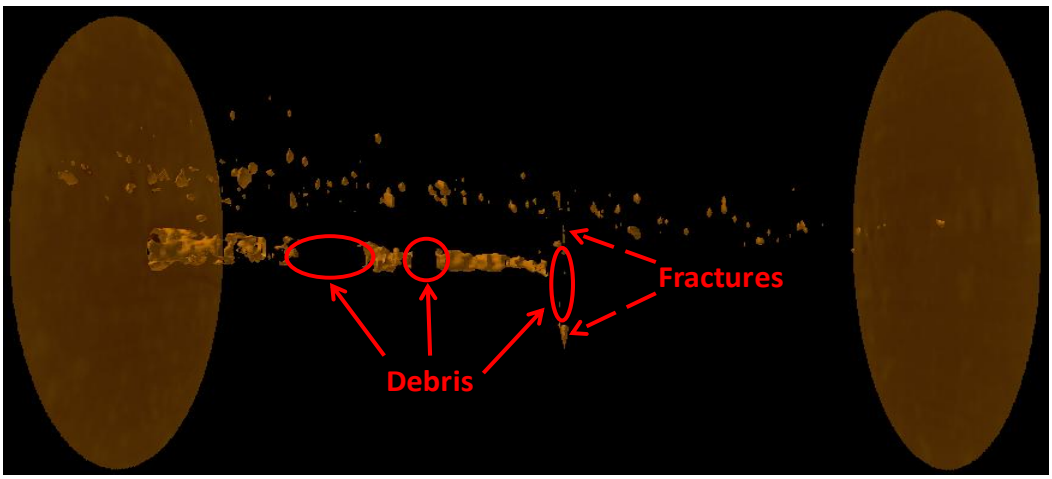

Fig. 9—3D Image of Core 2 – reactive charge.

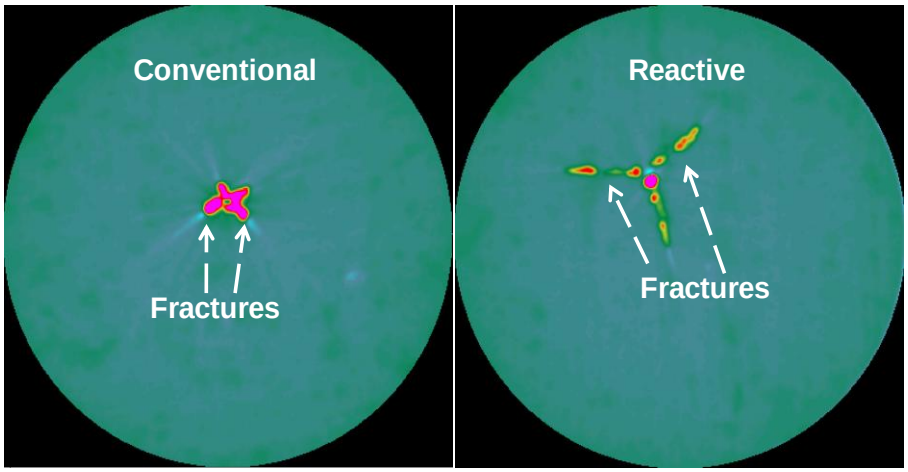

Fig. 10—Comparison of the fractures at the tip of the perforations.

Cores 3 and 4 were perforated using 7 gram charges as well, but they were perforated at an overbalanced condition with a 500 psi overbalanced pressure. The results are very similar to the first two cores. Debris are observed in both cores, the fractures at the tip of the tunnels are longer in core 4, and the volume of the perforation tunnel in core 4 is larger as well.

Cores 5 and 6 were perforated at a balanced pressure condition but using 12 gram charges. The results are very similar to the previews cores, but core 5 which was perforated with a conventional charge has a perforation tunnel that is 2.3 inches longer than the perforation in the core perforated with a reactive charge (core 6). After evaluating the initial images of the perforated core samples before acidizing, the core flood experiments were carried out. **Table 2** shows a summary of the results obtained. Even though vugs were noticed in the CT images, the initial rock properties such as permeability and porosity are similar; this allows the comparison of the results. As mentioned before, oil is first pumped at 10 cm^3 /min until steady state flow is reached to evaluate the injectivity of the core samples. Comparing the first two experiments (cores 1 and 2), even though core 1 has a higher initial permeability, the injection pressure in the core 2 test is lower, which means that the reactive charge (core 2) provided a more efficient and cleaner perforation tunnel. As reported by Bartko et al. (2007), higher injectivity would help to propagate more dominant wormholes. This observation was also noticed in our experiments. **Figs. 11 and 12** show the 3D CT images of these two cores. The core perforated with a reactive charge (core 2) provided more dominant wormholes, which resulted in slightly less acid to breakthrough.

Table 2—Core flood experiments' results

Test Number	Original Rock Permeability, md	Porosity, fraction	Injection ΔP, psi	Acid to Break through, ml	Acid to Break through, PV
Core 1	5.29	0.257	375	95	0.1851
Core 2	3.48	0.256	351	91	0.1802
Core 3	2.67	0.254	365	87	0.1712
Core 4	2.89	0.256	298	85	0.1706
Core 5	3.95	0.259	224	56	0.4605
Core 6	2.58	0.258	288	63	0.2589

The initial rock permeability of cores 3 and 4 are very similar, but core 4 which was perforated with a reactive charge showed higher injectivity. The results of these two cores are consistent with the results obtained from cores 1 and 2, with slightly less acid needed to breakthrough core 4.

The results obtained from cores 5 and 6 do not provide any further information in terms of the relation between injectivity and acid volume to break through, because the lengths of the perforation tunnels are considerably different. But it can be observed that the acid pore volume needed to break through core 6 is significantly lower than the pore volume needed in core 5, meaning that wormholes propagation was more efficient in the core perforated with the reactive charge. It is important to remember that the term "acid pore volume to break through", is the ratio of the acid volume used to break through over the core pore volume from the tip of the perforation to the outlet. It can also be observed that the difference in acid pore volume to break through is more evident or significant in these two cores than in the previous experiments. It is believed that the explanation for the results obtained from the last two experiments is that these cores were perforated with bigger charges (12 gram charges), meaning that the reactive

charge had more reactive materials to clean the perforation than in the previous experiments where 7 gram charges were used.

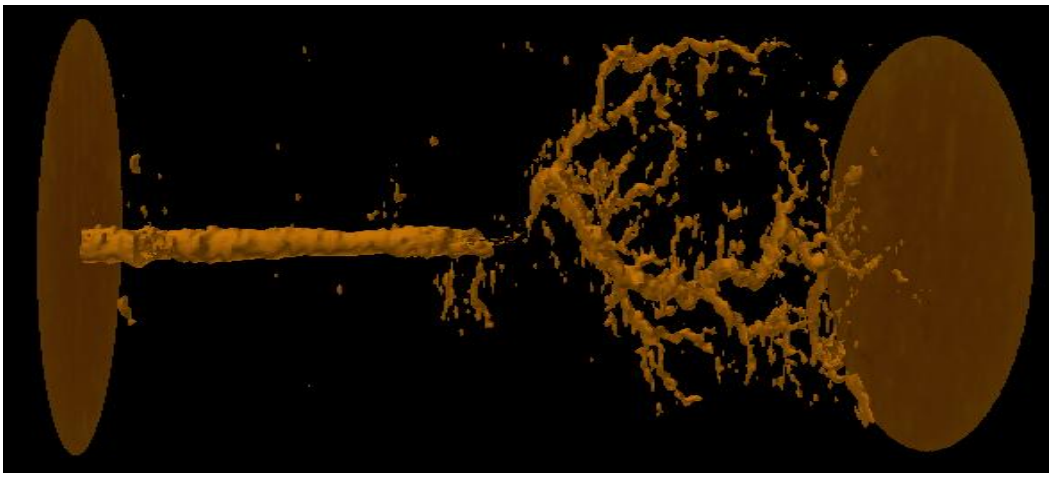

Fig. 11—3D Image of Core 1 test after acidizing.

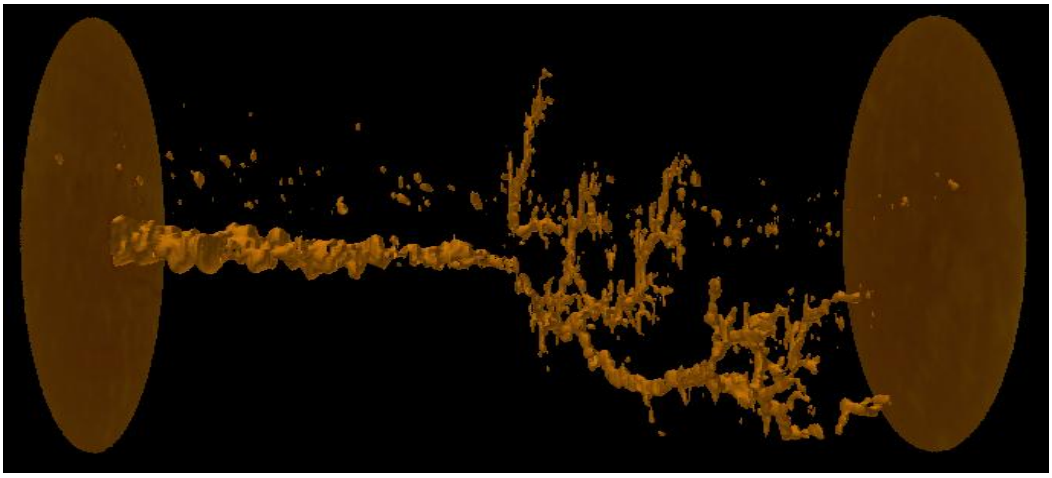

Fig. 12—3D Image of Core 2 test after acidizing.

Fig. 13 shows the results obtained from the compositional analysis of the fluid samples collected in the core 1 test. The acid behaves like a piston displacing the oil in the core. This event is confirmed by the samples shown in **Fig. 14**, since acid is observed coming out of the system after it breaks through the core (sample 13). This data was then correlated with the pressure data to confirm the exact time that acid breaks through the core, which was used to estimate the acid volume needed to break through. It can also be observed in Fig. 14 a dark layer on top of the acid in samples 13, 14, and 15, this is debris that are removed from the perforation tunnels by the acid flow, this observation confirms the presence of debris in the cores before acidizing. The results obtained in the rest of the experiments are very similar to the results from core 1 test, thus they are not reported.

Fig. 15 shows the fluid samples collected during the flow back of core 1 test. It can be observed that there is not debris present in these samples, meaning that debris is removed from the perforations by the acid. This samples didn't provide any further information, thus the flow back samples collected from the rest of the experiments are not reported, since the results are the same.

To sum up, it can be said that perforation tunnels obtained with reactive charges showed higher injectivity, this fact was confirmed by the results obtained in terms of acid pore volume to breakthrough. It is known that wormholes propagation is dependent on the acid flux, therefore; it is believed that reactive charges provide cleaner perforations, which increases the acid flux at the tip of the perforation and at the same time helps to propagate wormholes more efficiently.

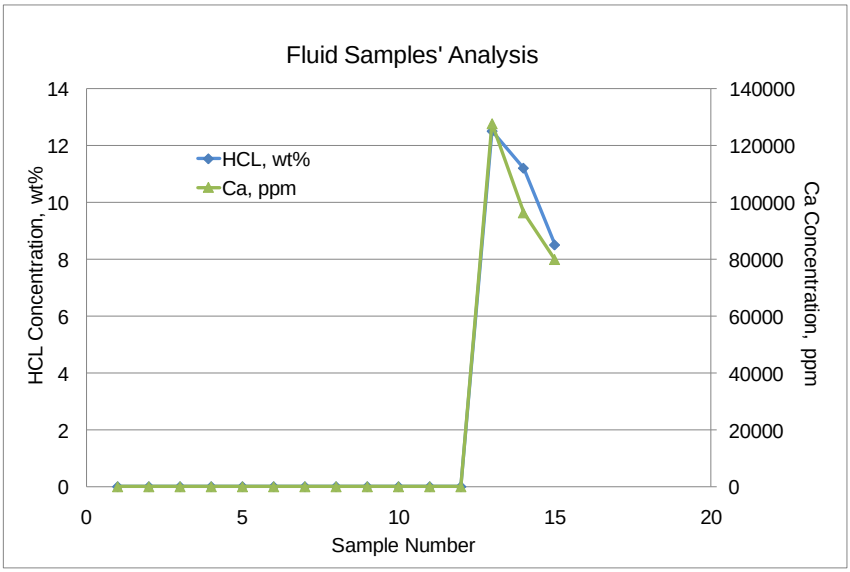

Fig. 13—HCL and Ca concentration Core 1 test.

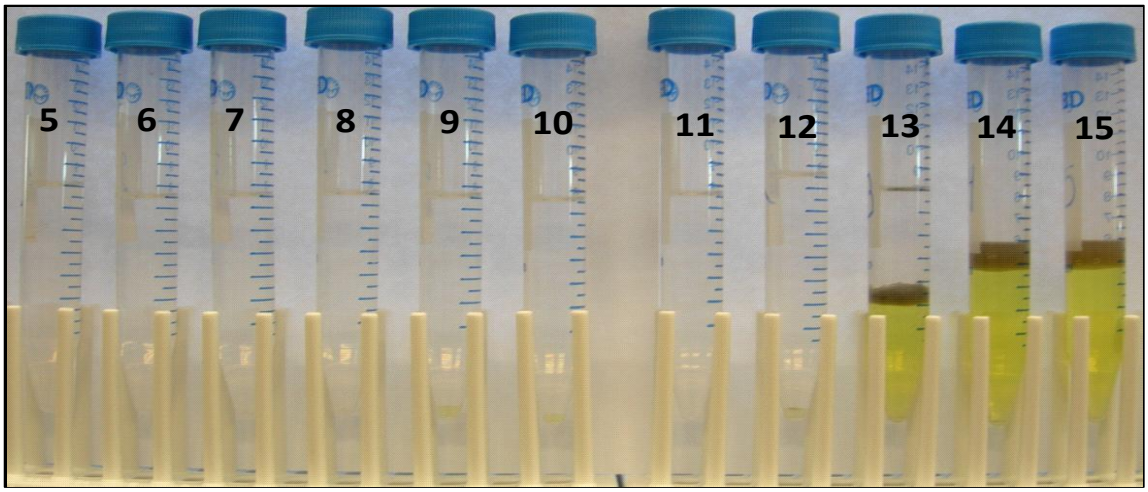

Fig. 14—Picture of fluid samples obtained in Core 1 test.

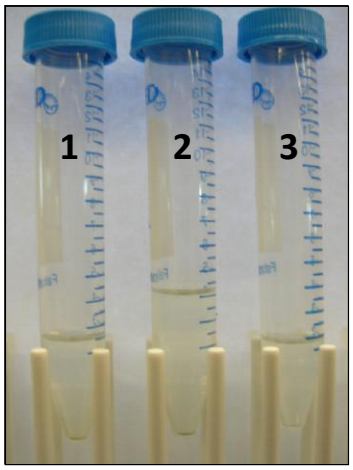

Fig. 15—Picture of flow back fluid samples obtained in Core 1 test.

Conclusions

After finalizing this research work and observing the results obtained from the perforated cores and core flood experiments, the resulting conclusions are:

- Reactive charges created perforation tunnels with higher injectivity. Higher injectivity perforations can be an important advantage for stimulation jobs, flow performance, and well productivity.
- The CT scan images and effluent fluid samples confirmed the presence of debris in the cores perforated with conventional and reactive charges. It was not possible to quantify the amount of debris in the perforations, thus further research should be carried out to measure the concentration of the liner's materials in the fluid samples. This step would provide a better estimation of the cleaning efficiency obtained when perforating with reactive charges.
- The increase in injectivity provided by the reactive charges results from the cleaning and fractures created at the tip of the perforations. Even though liner's debris is still observed in the cores perforated with reactive charges the higher injectivity observed in the cores perforated with reactive charges compared with perforations of the same lengths created with conventional charges shows that less residual perforation damage was created by the reactive charges.

Wormholes propagated slightly more efficiently (smaller porevolume to breakthrough) in the cores perforated with reactive charges than in those perforated with conventional charges.

Acknowledgements

The authors would like to thank GEODynamics' management for providing the funding to conduct this experimental work, and collaboration to present this paper. The authors would also like to thank Mohamed Mahmoud who is a PhD candidate at Texas A&M University, for running the chemical analysis of core effluent fluids.

References

Handren, P.J., T.B. Jupp, and J.M. Dees, Oryx Energy Co., "Overbalance Perforating and Stimulation Method for Wells", SPE 26515, 68th Annual Technical Conference and Exhibition of the Society of Petroleum Engineers, Texas, 3-6 October 1993.

Bartko, K.M., Chang, F.F., Behrmann, L.A., and Walton, I.C.: "Effective Matrix Acidizing in Carbonate Reservoir-Does Perforating Matter?", SPE 105022, 15th SPE Middle East Oil and Gas Show, Bahrain, 11-14 Mar 2007.

Bell, M.R.G., Hardesty, J.T., Clark, N.G.: "Reactive Perforating: Conventional and Unconventional Applications, Learnings and Opportunities", SPE 122174, SPE European Formation Damage Conference, Netherlands, 27-29 May 2009.

Behrmann, L.A., Hughes, K., Johnson A.B. and Walton, I.C.: "New Underbalanced Perforating Technique Increases Completion Efficiency and Eliminates Costly Acid Stimulation", SPE 77364, SPE Annual Technical Conference and Exhibition, Texas, 29 September-2 October 2002.

Lloyd Stutz, H., Behrmann, Larry A., "Dynamic Under Balance Perforating Eliminates Near Wellbore Acid Stimulation in Low-Pressure Weber Formation", SPE 86543, SPE International Symposium and Exhibition on Formation Damage Control held in Lafayette, Lousiana,18-20 February 2004.

Cocanower, R.D., "Perforating Assumes New and Greater Importance in Well Stimulation", SPE 799, Mechanical Engineering Aspects of Drilling Production Symposium in Fort Worth, Texas, 23-24 March 1964.

Wang, Y., Hill, A.D., and Schechter, R.S., "The Optimum Injection Rate for Matrix Acidizing of Carbonate Formations", SPE 26578, 68th Annual Technical Conference and Exhibition of the Society of Petroleum Engineers, Texas, 3-6 October 1993.

Economides, Michael J., Hill, A. Daniel, and Economides, Christine E., "Petroleum Production Systems", 1994.